Ann. Rev. Astron. Astrophys. 1988. 26: 245–294

VOIDS

H. J. Rood

P.O. Box 1330, Princeton, New Jersey 08542

1. EARLY EXPLORATIONS

1.1 *Voids in Astronomy*

In the fifth century B.C., Democritus postulated the existence of immutable atoms characterized by size, shape, and motion. Changes in the combination of these atoms were postulated to result in the qualitative changes observed in everyday matter. In order to make the motions of atoms possible, the existence of the void (unoccupied space, empty space) was required [cf. 15th edition of the Encyclopaedia Britannica (1985)].

In astronomy, it is likely that individual voids were first observed by prehistoric man, who saw distinct dark regions within the prominent luminous band (now called the Milky Way) stretching across the sky. Although to the unaided eye these dark regions may seem devoid of light, on well-exposed photographs they appear dark only in contrast to their luminous starry neighborhoods. Counts, magnitudes, and colors of the few stars that lie within the boundaries of the dark regions imply the presence of vast quantities of obscuring particles (dust). The Coalsack is an example of a dust void in Galactic stellar astronomy (29, pp. 166–78; 141).

A typical "void" in the surface distribution of a sample of stars is not empty; it is a region where the stellar surface density is substantially smaller than that of (*a*) its surrounding (large local density contrast) or (*b*) an average over the entire sample of stars (large global density contrast), where the calculation of the average includes corrections for the selection functions of the sample. In *Galactic stellar* astronomy, a typical void in the surface distribution of stars corresponds to a region of three-dimensional space with an atypically large density of obscuring material. In *extragalactic* astronomy, the three-dimensional region that constitutes a void is transparent and empty or nearly empty of galaxies. Voids were not immediately recognized in the surface distribution of galaxies because

0066–4146/88/0915–0245$02.00

they tend to be overlaid by superimposed background and especially foreground galaxies. Voids were recognized only after Doppler velocities were measured for *statistically homogeneous* samples of galaxies in selected solid angles of the sky, which provided (through application of the Hubble relation between distance and redshift) direct information on the three-dimensional distribution of galaxies.

In extragalactic astronomy, the basic material unit is a galaxy with a characteristic length $D_c \sim 20$ kpc that typically moves within a group or cluster ($D_c \sim 50$ kpc–5 Mpc) in a supercluster ($D_c \sim 50$ Mpc or larger). (Herein, a length calculated from an angular extent and Hubble distance has been normalized with an adopted Hubble constant $H_0 = 50$ km s^{-1} Mpc^{-1}.) [Work on detecting and deciphering the structure of groups and clusters of galaxies (including discussion of the problem of the "missing mass") has been reviewed by Bahcall (10), Rood (156), and Sarazin (169).] The latter two reviews briefly discuss superclusters. A comprehensive review of research on superclusters is given by Oort (128). Superclusters and voids are often discussed together because (*a*) they are identified and studied with a common data base, and (*b*) it is likely that they share a common origin and represent two complementary effects of related physical evolutionary processes. Therefore, the present review refers frequently to Oort (128), and figures therein.

If the physical universe is modeled as one vast system of individually distinct galaxies, then these galaxies are immersed in one void, an analog of the void of Democritus. We obtain a similar result if the Universe is modeled as one vast system of groups and clusters of galaxies. However, research on superclusters is in such an early stage that it is not yet clear whether they are typically (*a*) individual entities immersed in the void (i.e. analogs of Democritus' atoms–galaxies, and groups and clusters of galaxies), or (*b*) parts of one vast system of galaxies that is polka-dotted in three-space with individual voids [analogous to the voids in two-space of Galactic stellar astronomy, but with a much larger fraction of the volume occupied by the voids (large polka dots)], or (*c*) parts of a connected structure of galaxies intertwined with a connected structure of voids. Models (*a*) and (*b*) are discussed in depth by Shandarin & Zel'dovich (176), and model (*c*), a spongelike universe, is described in detail by Gott et al. (80).

Pending clarification of the topological nature of superclusters and voids, which may require the completion of the Center for Astrophysics (CfA) redshift survey of galaxies with apparent photographic magnitude $m_p \leq 15.5$ [where the adopted m_p is generally the Zwicky (220) magnitude; see (93a) for discussion of comparisons between Zwicky magnitudes and other, more accurate but less abundant blue magnitudes], it is often useful

to think of a void as a discrete entity—a region containing significantly fewer galaxies than predicted by the appropriate Poisson distribution. The occurrence of physical groupings of galaxies evidently *requires* the presence of voids defined in this way.

There are two ways that an individual void can be studied observationally: (*a*) The void can be probed with telescopic sensors in attempts to detect something within it. (*b*) The structure and content of the contiguous *shell of superclusters* surrounding the void can be studied. [The term "shell" has been adopted from de Lapparent et al. (56). M. Postman (private communication, 1987) suggests that "shell of galaxies" may be a more appropriate term, as it is not yet clear that superclusters are physically correlated.]

1.2 *Technological Prerequisites*

Early surveys of galaxies over large solid angles of the sky indicated to a number of astronomers (including William and John Herschel, Lundmark, Holmberg, Shapley, Oort, de Vaucouleurs, Shane & Wirtanen, and Abell) the superclustering of galaxies, i.e. the predominant occurrence of galaxies, groups, and clusters within larger structures now called superclusters (cf. 5, 58, 92a, 113a, 128, 142, 158a, 178). Zwicky interpreted cluster cells as the space fillers of the cosmos (219a). In contrast, from independent counts of galaxies to faint magnitudes in a large number of small survey fields distributed over the sky, Hubble concluded that groups and clusters of galaxies are aggregations drawn from the general field, which is everywhere and in all directions approximately uniform (93, pp. 72, 81–82). To discriminate between these models, we need to know the three-dimensional distribution of galaxies in large homogeneous samples. To an approximation that neglects the peculiar motions of galaxies, distances can be estimated from redshifts, using the Hubble relation between redshift and distance. The observational requirement reduces to obtaining redshifts from Doppler-shifted spectral lines of the galaxies in large homogeneous samples.

In the 1920s it took several nights of observation to accumulate the necessary exposure time for the spectrographic determination of the redshift of a bright galaxy. By the mid-twentieth century, the sensitivity of photographic emulsions had increased to the extent that with the nebular spectrograph of the 36-inch Crossley reflector at the Lick Observatory, N. U. Mayall could determine the redshift of a luminous galaxy in the Coma cluster with an exposure of five hours. By 1960 Mayall had identified a homogeneous sample of 83 bright galaxies in a field of the Coma cluster of solid angle $\simeq 33$ sq deg (116, Figure 1), and had measured the redshifts of 50 galaxies in this sample. Mayall's (116, Figure 2) plot of redshift vs.

radial distance from the center of the Coma cluster is depicted in Figure 1. Mayall recognized that the development of electronic photography pioneered by A. Lallemand, in which the intensity of an image is amplified electronically before it is recorded on a light-sensitive emulsion, would usher in a new era of extragalactic spectroscopy (116). By the late 1960s, a device of this type, the Carnegie image-tube, reduced the exposure time for each of the remaining galaxies in Mayall's sample to $\simeq 30$ min, and the redshift survey was completed (161).

Although electronic photographic spectroscopy reduced exposure times immensely, the spectrum of a galaxy along with the night sky was still registered on a photographic plate, and tedious hours were spent measuring the plate for final reduction with a digital computer. The Doppler velocity was derived from the measured shift of the few strongest spectral lines, and the accuracy achieved was typically ± 100 km s^{-1} for absorption lines and ± 50 km s^{-1} for emission lines (157). Early work on superclustering of galaxies (Section 1.3) was done primarily with these techniques, and the postobservation reduction time tended to limit these studies to samples of ~ 100 galaxies in regions of the sky covering only ~ 30–300 sq deg.

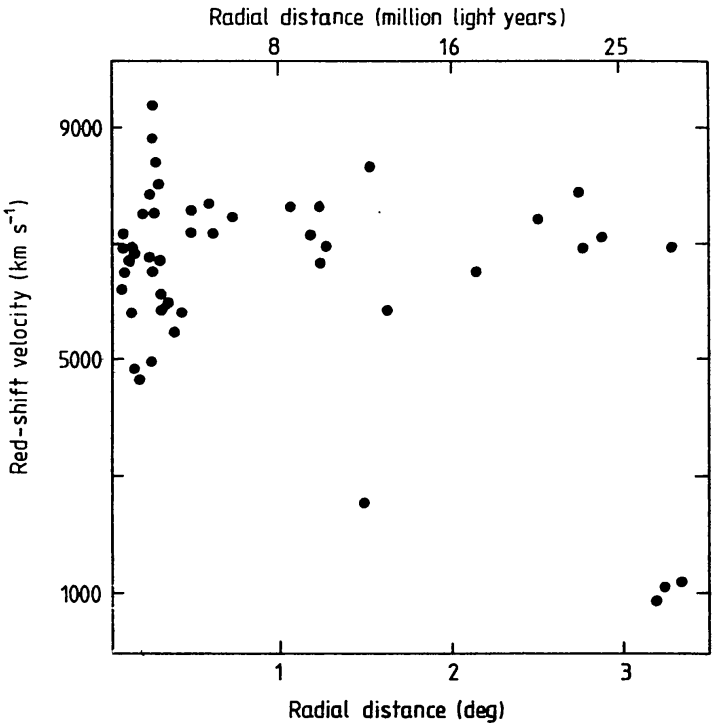

Figure 1 Doppler velocity (derived from observed redshift) vs. distance (on the sky) from the center of the Coma cluster for the 50 galaxies in the sample by Mayall (116). The Coma cluster is part of a structure that extends to >8 Mpc (25 million lt-yr). Note the large empty region in the foreground. Adapted from Figure 2 of (116).

Finally, in the 1970s, equipment was developed by, e.g., Shectman & Hiltner (181, and references therein) that, at the telescope, continuously subtracts off the contribution from the night sky, electronically integrates the spectrum during the exposure, and then transfers the sky-subtracted spectrum directly onto a magnetic tape for computer utilization, where the final reductions can be performed quickly and as automatically as desired. Current observational studies on superclustering of galaxies (Section 2.1) are done primarily with these electronic spectroscopic techniques and with the complementary automatic techniques provided by 21-cm spectral-line radio astronomy. With modern reduction techniques (described below) applied to the spectral data of electronic spectroscopy, Doppler velocities are derived with a typical accuracy of ± 30 km s^{-1} independent of the mix of absorption and emission lines in the spectrum. The techniques of 21-cm astronomy achieve typical accuracies of ± 10 km s^{-1} (60, 157).

The 1974 paper by Susan Simkin (183) marked a watershed between (*a*) the early technique of measuring the Doppler velocity of an individual galaxy from the locations of a few strong lines of a sky-contaminated spectrum and (*b*) the modern technique of applying Fourier transform (172) or cross-correlation (197a) techniques to obtain the Doppler velocity that provides the best match between a sky-free absorption-line spectrum and that of a well-constructed zero-redshift templet spectrum. Simkin introduced the new techniques, described many of their advantages, and presented a mathematical apparatus to determine both the systemic Doppler velocity and the internal Doppler velocity dispersion of a galaxy. The accuracy achieved in a determination of the Doppler velocity of a galaxy by 21-cm and modern optical techniques (± 10–30 km s^{-1}) permits the determination of the internal Doppler velocity dispersion of (*a*) individual galaxies (typically ~ 100–300 km s^{-1}) and (*b*) small groups of galaxies [typically ~ 130 km s^{-1} (214)] (Section 4.2).

1.3 *A Hidden Paradigm*

As noted above, early studies of the surface distribution of galaxies featured three different models: (*a*) superclustering of galaxies, (*b*) super-large rich clusters, and (*c*) groups and clusters drawn from a uniform general field. In order to discriminate between these models and to relate the data to predictions of physical models of the growth of structure in the Universe, Peebles and coworkers (69a, 142) extracted the amplitude and slope of the correlation function from large sets of data on the surface distribution of galaxies (cf. Section 3.1.2). They found that galaxies and systems of galaxies are correlated on all scales up to the noise limit of their analyses, between ~ 10 and 100 Mpc. The results are consistent with (*a*) and (*b*) but not with (*c*).

Nevertheless, model (*c*) remained popular. In 1975 Turner & Gott (205) analyzed the surface distribution of galaxies with apparent blue magnitude $m_p \leq 14$ and found that if the galaxies are separated into two classes, A (associated) and S (single) [terminology by (187)], according to whether the nearest neighbor on the sky lies within or beyond 45 arcmin, respectively, then the galaxies in set A (60% of the total) display the correlation function found by Peebles and coworkers, but the galaxies in set S (40% of the total) exhibit no correlations among themselves and are identified as a homogeneous (i.e. almost uniform) population of galaxies (205). However, in 1977, Soneira & Peebles (187) studied the problem more thoroughly and found that (*a*) the galaxies in set S are in fact clustered among themselves and with the galaxies in set A, (*b*) the S and A galaxies show strong and similar correlations with fainter galaxies, (*c*) the large-scale clustering of the galaxies in sets S and A are quite similar, and (*d*) the observational data agree well with simulation data of a hierarchical model of structures with no homogeneous field population; Soneira & Peebles concluded that if a field component of galaxies does exist, it accounts for substantially less than 10% of the galaxies in a catalog selected by apparent magnitude. This result was confirmed in a recent analysis by Vettolani et al. (207b, 209) of the three-dimensional distribution of galaxies with $m_p \leq 14.5$ covering a large solid angle in the sky, which failed to detect a nonclustered homogeneous background of galaxies.

In September 1975, a paper by Chincarini & Rood appeared in the journal *Nature* that presented results of a nearly complete homogeneous survey of redshifts of galaxies with $m_p \leq 15.0$ in a 30 sq deg region west of the center of the Coma cluster (45). A graph was published that suggested to the authors that galaxies are associated with the Coma cluster to a radial distance of at least 32 Mpc (Figure 2). This extended the directly measured radial extent of the associated galaxies by a factor of 4 beyond that evident in the tantalizing original plot by Mayall (116, Figure 2) (depicted in Figure 1) and an updated version discussed with model extrapolations (161, Figure 1). This result suggested to the authors that the Coma cluster (radial extent ≥ 32 Mpc) is larger than the Local Supercluster. They also mentioned that such a large radius implies that gravitational mixing between the inner and outer regions is not well advanced, so that the properties of the outer regions reflect to a significant extent the initial conditions of the cluster formation period. J. H. Oort (private communication, 1975) pointed out that our observed and deduced properties of the structure more consistently indicate that it is a supercluster containing the Coma cluster. And P. J. E. Peebles (private communication, 1975) noted the consistency between (i) our direct detection of large-scale correlations to radii > 30 Mpc among the galaxies in a three-

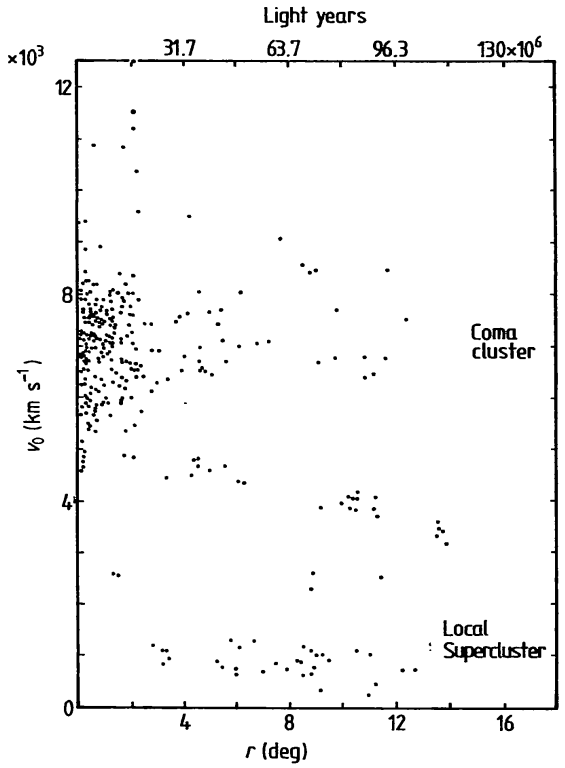

Figure 2 Doppler velocity vs. observed radial distance from the center of the Coma cluster for the galaxies in the sample by Chincarini & Rood (45). The Coma cluster is part of a structure that extends to >30 Mpc (100 million lt-yr). Note the large empty region in the foreground. Adapted from Figure 1 of (45).

dimensional sample of small solid angle, and (ii) similar recent results from analyses of correlation functions derived from the surface distribution of galaxies over large solid angles of the sky. The evidence was fast accumulating that the Universe conforms to model (*a*), the superclustering of galaxies.

The stream of research that led to (45) (*a*) began in 1960 with Mayall's far-reaching paper on electronic photographic spectroscopy (116); (*b*) continued in September 1969 with a remark by T. W. Noonan (private communication, 1969) that the rich cluster A1367 may be associated with the Coma cluster because they have the same Abell richness and distance class and are only 20° apart on the sky; (*c*) continued in the late 1960s with the application of the Carnegie image-tube spectrograph on the 2.1-m telescope at Kitt Peak National Observatory to complete the redshift survey begun by Mayall, and with the application of the data to a comprehensive study published in 1972 on the structure of the Coma cluster (161); and (*d*) continued in the late 1960s and early 1970s with the determination of large numbers of redshifts of galaxies in clusters at a rate of >10 per

night of observation (a realization of Mayall's vision) (43a), and with the publication in 1972 of initial results from the redshift survey for the 30 sq deg region west of the Coma cluster [selected to simultaneously (i) extend Figure 1 to larger radial distances, (ii) make significant, albeit leisurely headway toward A1367, and (iii) decipher the nature of the survey field that Zwicky et al. (220) identified as Cluster No. 16 in Field No. 158] (44). The data and analytical techniques that provided the bases for the discussion in (45) were published more fully in November 1975 (153a) and May 1976 [(46), but with most of the new data mistakenly placed by the printers in (95)]. This work, in major respects, was superseded in 1978 with the publication by Gregory & Thompson (81) of results obtained from their redshift survey of galaxies in a region that spanned completely from the Coma cluster to A1367. It independently occurred to Gregory & Thompson (from evidence similar to that which led Noonan to a similar insight at least six years earlier) that the Coma cluster and A1367 are likely to be part of a common physical entity. Gregory & Thompson constructed their observing program to test this hypothesis, obtained the necessary new data in one observing run, and then wrote the benchmark paper that clearly presented the observational evidence demonstrating the existence of (*a*) the Coma/A1367 supercluster with a characteristic length >40 Mpc and (*b*) a foreground region apparently devoid of galaxies with a characteristic length >40 Mpc (81). The discussion and Figure 2 of (81) [= Figure 12 (p. 391) of Oort (128)] provided a significant catalyst for motivating extragalactic astronomers into action. Observational workers began a dedicated and systematic attack on the problem of determining the direct three-dimensional distribution of galaxies by applying efficient and accurate analytical techniques to the data of modern detector and computer technology (Section 2.1). And theoretical workers began to use results from the new data to constrain parameters in old, revised, and new models invented for the purpose of explaining the astrophysical origin and evolution of large-scale structure in the Universe.

During the early 1970s, Chincarini and I were accumulating new galaxy redshifts to study the structure of a Zwicky cluster (220) in the constellation Hercules, which contains three Abell clusters (A2147, A2151, and A2152) (4). In 1974, while examining the data accumulated up to that point, Chincarini noticed that the redshifts are segregated into a small number of groups. Because this also occurs in all of the relatively homogeneous samples of redshifts that we had obtained for other parts of the sky, he hypothesized that galaxies occur in groups (e.g. clusters and superclusters), and that the apparent field of galaxies in a surface distribution is the result of a superposition of such groups. [Chincarini & Martins (43), Focardi et al. (73)].

In 1976, efforts were intensified to complete the redshift survey for a homogeneous sample of galaxies in the constellation Hercules and to add a redshift survey for a homogeneous sample of galaxies in a contiguous region that extends from Hercules to the cD cluster A2199. Results were published in 1979–81 (37, 49, 191, 191a, 192). The distribution of points in plots of redshift vs. declination for these galaxies [Figures 17–19 (pp. 401–2) of Oort (128)] led to (*a*) the definitive demonstration of the reality of a supercluster that connects the triplet of Abell clusters in Hercules (A2147, A2151, A2152) to A2199 [Abell had suggested the existence of this supercluster as early as 1961 (5)], and (*b*) the discovery of a large void in its foreground, both with a characteristic length >50 Mpc. The stream of research that led to the discoveries of superclusters and voids from early redshift surveys of the Coma and Hercules regions was described in 1980 by Chincarini & Rood (48) and in 1982 by Gregory & Thompson (82). Perhaps the first use of the term "void" in the extragalactic literature occurred in (48) and the Hercules papers (191, 192) following a suggestion in 1979 by an individual at the University of Oklahoma, identity unknown. "Void" is in fact a natural contraction of "region devoid of galaxies," which had been used earlier (e.g. 81, 196). A summary of the discoveries from the early redshift surveys and a pioneering discussion of the statistics and characteristics of superclusters, their formation, and a possible relation of superclusters and voids to Lα absorption lines in quasars were presented in 1981 by Oort (127).

The superclustering of galaxies [model (*a*)] and the presence of voids are now accepted as fact, a paradigm among workers on large-scale structure. I have suggested that 1975 was a pivotal year in the birth of this paradigm, which to a large extent replaced Hubble's model (*c*); it is fascinating to identify elements of model (*c*) in the analyses and discussions within papers written around that time (e.g. 53, 126a, 154, 165, 166). The latter two papers, published in 1976 by Rubin et al., are especially interesting. For a homogeneous sample of Sc I, II galaxies, (*a*) the distances derived by assuming that the galaxies are "standard candles" (each with the same absolute blue luminosity) and (*b*) the distances inferred from their redshifts through the Hubble relation were found to display slightly different systematic variations across the sky consistent with a 454 ± 125 km s^{-1} motion of the Local Group relative to the reference frame defined by the galaxies. The literature contains discussions of the influence on derived standard-candle distances of systematic errors caused by, e.g., effects of superclustering and Malmquist bias (cf. 70, 83, 164a, 210c), but a recent study that analyzes subsets of the Rubin et al. sample by correcting for systematic biases and applying independent distances derived from, e.g., red and infrared luminosities and absolute luminosities inferred from H I 21-cm

velocity widths through the Tully-Fisher relation suggests that the effect represents real motion (50a).

On September 12–16, 1977, IAU Symposium No. 79 was held in Tallinn, Estonia, USSR. There I learned that as early as 1970, Ya. B. Zel'dovich and coworkers were evolving theoretical models showing that interesting large-scale structure (e.g. Figure 3) was formed by nonlinear dissipative collapse of gaseous density perturbations, forming "pancakes," followed by condensation into galaxies (215, 215a, 215b, 217). In contrast, many cosmologists in the West assumed that galaxies formed initially by Jeans instabilities within random density perturbations that evolved into a hierarchy of larger structures that could be tracked by *N*-body computer experiments [cf. (2a, 187a, 205b) and Figure 26 (p. 424) of Oort (128)]. By analyzing the heterogeneous data in the literature, including the new homogeneous data from redshift surveys discussed above, Einasto and coworkers (e.g. 99a) found that the observed large-scale three-dimensional distribution of galaxies exhibits cellular structure with remarkable qualitative similarity to the model realizations of Zel'dovich et al., but not to results of random gravitational clustering. These suggestive general conclusions were consistent with the discoveries of superclusters and regions "devoid of galaxies" obtained from redshift surveys of homo-

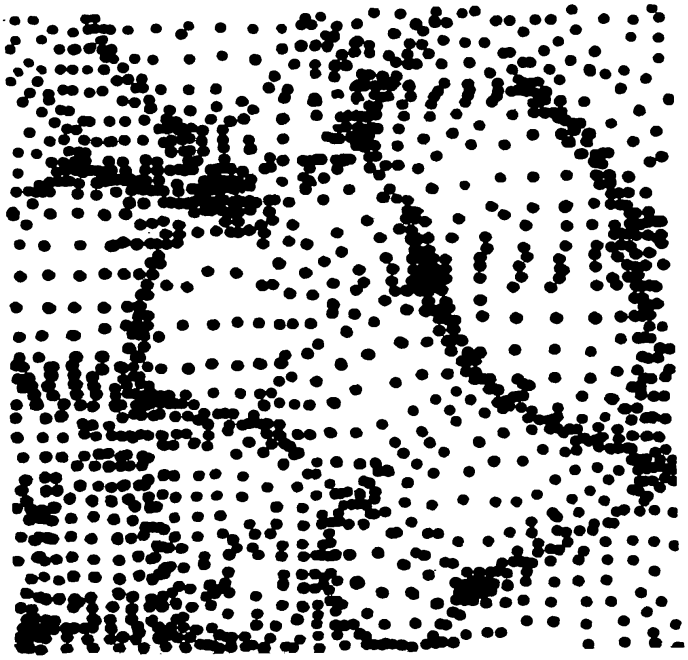

Figure 3 A realization of large-scale structure that has evolved from initial gaseous density perturbations that undergo nonlinear dissipative collapse. This figure, the result of calculations by Zel'dovich & Novikov (217), was presented at IAU Symposium No. 79 held on September 12–16, 1977, in Tallinn, Estonia, USSR (215b).

geneous samples of galaxies in selected regions of the sky that were reported by observers from the US (191a, 196a).

In 1981, Ikeuchi (98) and Ostriker & Cowie (133) suggested that cosmic explosions with an energy release $\sim 10^{61}$ ergs originating from, e.g., quasars or young galaxy starburst events would create blast waves that might be influential in promoting, or amplifying, galaxy formation, and that might also produce large-scale structure by tending to create voids with outward-moving galaxies on their contiguous shells (130). In summary, by 1981 the astrophysical inventory of known mechanisms that tend to generate large-scale structure had grown to include (*a*) gravitational mechanics of galaxies, (*b*) dissipative gravitational collapse of gaseous density perturbations, and (*c*) blast waves from cosmic explosions.

2. INDIVIDUAL VOIDS (CURRENT OBSERVATIONAL STUDIES)

2.1 *Results From Galaxy Redshift Surveys*

Previous reviews of this topic include those by Chincarini (38, 39), Doroshkevich et al. (62), Geller et al. (79a), Oemler (126b), Schwarzschild (175), Shandarin & Zel'dovich (176), and Zel'dovich et al. (216). The review by Geller et al. (79a) contains information in addition to that below.

2.1.1 IDENTIFICATION AND STRUCTURE OF VOIDS The early Coma/A1367 redshift survey (81) covers 260 sq deg. The sample of galaxies is nearly complete to $m_p \simeq 15$ corresponding to an effective Doppler velocity limit $V_{lim} \sim 8000$ km s^{-1}. The early Hercules/A2199 redshift survey (49) covers a 332 sq deg region. The sample of galaxies was drawn *randomly in location and apparent magnitude* from a population complete to $m_p \simeq 15.5$ ($V_{lim} \sim 11{,}000$ km s^{-1}). Both surveys revealed a prominent void with a characteristic length >40 Mpc. These voids were detectable because they are small compared with the effective depth of each survey ($\sim$160–220 Mpc).

Although redshifts have been measured for the galaxies in the all-sky Shapley-Ames survey (59b, 167a) complete to $m_p \simeq 13$ (i.e. $V_{lim} \sim 3000$ km s^{-1}), the effective depth ($\sim$60 Mpc) and the location of our Local Group of galaxies within the Local Supercluster precluded the discovery from these data of any obvious void with characteristic length >40 Mpc. Because of these same survey properties, however, the data on Shapley-Ames galaxies have contributed greatly toward increasing our knowledge of the structure of the Local Supercluster, and Tully (202), 203) [papers reviewed by Oort (128), pp. 380–384] finds that the great majority of

galaxies in the supercluster are located in nine "clouds," with most of the space between empty.

Although the redshift surveys covering small solid angles of the sky led to pioneering discoveries of individual voids (e.g. Coma/A1367, Hercules/A2199), redshift surveys covering large solid angles of the sky are necessary to obtain statistical information on the locational and physical properties of voids in general, as well as to obtain more complete structural information about individual voids and their contiguous shells. The data from the CfA redshift survey of the 2400 galaxies complete to $m_p = 14.5$ with $b > 40°$, $\delta > 0°$ and $b < -30°$, $\delta > -2.°5$ [where b is Galactic latitude and δ is declination (epoch 1950)] have been published (93a), and initial results (59c) have been reviewed by Oort (128, pp. 385–94). Significant progress has been made toward the completion of a corresponding redshift survey of the >12,000 galaxies in the same solid angle of the sky with $m_p \leq 15.5$ (J. Huchra, preprint, 1987); for example, initial results from part of this survey (discussed below) are beautifully illustrated by de Lapparent et al. (56) as reproduced in Figure 4. Da Costa et al. (51b) have carried out a complementary redshift survey of 1963 galaxies that is 84% complete (redshift measurements obtained for 1657 galaxies) to an angular diameter limit of 1 arcmin (very roughly $m_p \sim 15$) in 1.75 ster of the southern sky ($\delta \leq -17.°5$, $b \leq -30°$).

The early studies described in Section 1.3 established that the void in the foreground of the Coma/A1367 supercluster spans at least from the Coma cluster (A1656) ($\alpha = 12^h57^m$, $\delta = 28°15'$, $V = 6955$ km s^{-1}) to A1367 ($\alpha = 11^h42^m$, $\delta = 20°7'$, $V = 6446$ km s^{-1}) and that the void in the foreground of the Hercules/A2199 supercluster spans at least from the Hercules cluster (A2151) ($\alpha = 16^h3^m$, $\delta = 17°53'$, $V = 11{,}122$ km s^{-1}) to A2199 ($\alpha = 16^h27^m$, $\delta = 39°28'$, $V = 9264$ km s^{-1}), where the equatorial coordinates are for epoch 1950 and the Doppler velocity is relative to the centroid of the Local Group. Neta Bahcall (private communication, 1986) pointed out that these two voids are in fact segments of the two largest voids in Figure 4*a* from de Lapparent et al. (56), which I call the Coma/A1367 void (or "Coma void," for short) and the Hercules/A2199 void (or "Hercules void," for short). Figure 4*a* is a plot of Doppler velocity vs. right ascension (over a range of 9 h) for a nearly complete sample of galaxies with $m_p \leq 15.5$ in a 6° strip of declination that contains the Coma cluster. Figure 4*b* is the same as Figure 4*a* but with $m_p \leq 14.5$. Figure 4(*a*,*b*,*c*) [which supersedes Figures 11 and 12 (pp. 390–91) of Oort (128)] provides a clear demonstration of the detailed new structural information on voids that is obtainable from the CfA redshift survey to an apparent magnitude limit of $m_p = 15.5$ and demonstrates that the Coma and Hercules voids are much more well defined from data with a survey limit of

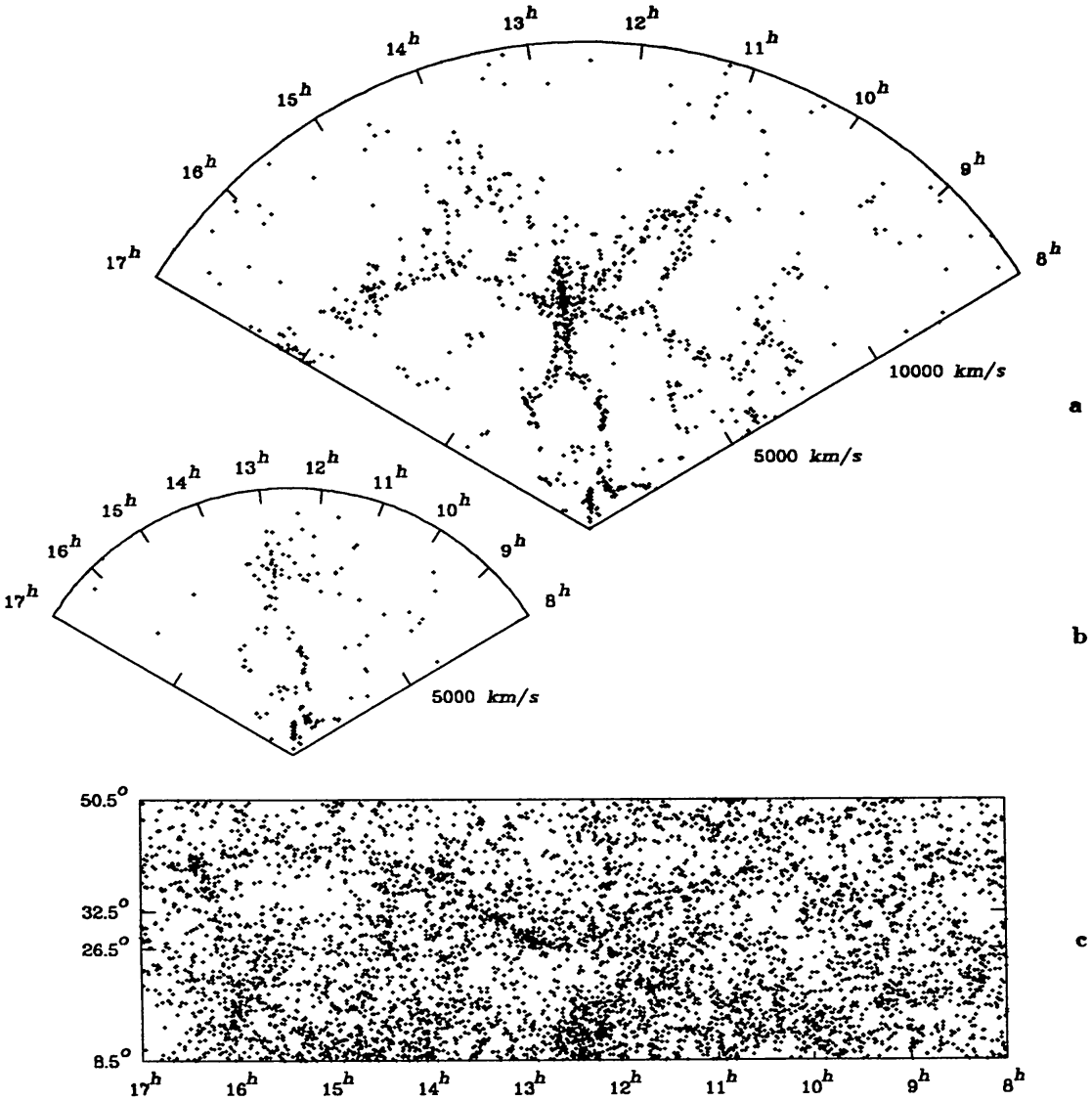

Figure 4 (*a*) Map of the Doppler velocity vs. right ascension in the declination wedge $26.°5 \leq \delta \leq 32.°5$. Data are plotted for 1061 galaxies with $m_p \leq 15.5$ and $V \leq 15{,}000$ km s^{-1}. (*b*) Same as Figure 4*a* for $m_p \leq 14.5$ and $V \leq 10{,}000$ km s^{-1}. Data are plotted for 182 galaxies. (*c*) Projected map of the 7031 objects with $m_p \leq 15.5$ listed by Zwicky et al. (220) in the region bounded by $8^h \leq \alpha \leq 17^h$ and $8.°5 \leq \delta \leq 50.°5$. Reproduced from (56) by permission of Margaret J. Geller.

$m_p = 15.5$ (Figure 4*a*) than from data with a survey limit of $m_p = 14.5$ (Figure 4*b*); this unequivocally demonstrates the physical reality of these voids with their contiguous shells—i.e. with improved statistics, these structures have risen significantly farther above the noise. [The reader may wish to assess quantitatively whether the statistical confidence level of this statement is actually tantamount to certainty; some considerations relevant to this problem are discussed in (57) and Section 3.1.]. De Lapparent et

al. (56, 57) note that the Coma and Hercules voids each have a characteristic length ~ 50 Mpc, and their contiguous shells are sharply structured. Part of the Local Supercluster with its effective Doppler velocity ~ 1000 km s^{-1} that is evident in Figure 2 is also apparent in Figure 4*a* as part of the contiguous shell of the Coma void. Because the angular extent of the Coma and Hercules voids are each $>6°$, de Lapparent et al., in order to obtain additional information on their structure, examined a map of the surface distribution of the galaxies with $m_p \leq 15.5$ in a strip with the same center and range of right ascension but with a width of 40° (Figure 4*c*). De Lapparent et al. suggest that the cellular pattern evident in Figure 4*a* and the smoothness of Figure 4*c* are simply understood if the galaxies are distributed on the surfaces of shells tightly packed next to each other. [It is remarkable that 10 yr earlier Einasto and coworkers were able to reach very similar conclusions from examination of the heterogeneous data available at that time (cf. 99a), albeit with some theoretical guidance by Zel'dovich et al. (cf. 215b, 217).]

The de Lapparent et al. study (56, 57) underlines the potential value for future work of (*a*) the entire CfA redshift survey complete to $m_p = 15.5$ over a large fraction of the sky and (*b*) the completed subset of data covering the 6° strip that was analyzed in (56, 57). [This data is being prepared for publication and will also be made available on magnetic tape for distribution by the Astronomical Data Center at the Goddard Space Flight Center (M. Geller, private communication, 1987)]. With (*a*), one should be able to establish with certainty whether the galaxy distribution is in fact cellular, filamentary, some combination of both, or something else. With (*b*), one could, e.g., subtract out the distorting effect of virial motions of galaxies, especially from the Coma cluster, to establish whether the Coma and Hercules voids are independent entities, or possibly, e.g., two parts of one void or the network of voids in the spongelike model of Gott and coworkers (cf. 80). And one could examine the declination of each galaxy with the same Doppler velocity and right ascension as a point in the interior of the Coma or Hercules void to determine whether the galaxy is nevertheless outside or actually within the void.

In 1978, Kirshner et al. (103) set out on a pioneering study of the deep-space distribution of galaxies. They obtained redshifts and direct photometric magnitudes for most of the galaxies (164 of 184) to a completion limit of $m_p \simeq 15.5$ ($V_{lim} \sim 11{,}000$ km s^{-1}) in eight representative square fields $\simeq 4°$ on a side, four in the northern and four in the southern Galactic hemisphere. They planned to redetermine the galaxy luminosity function and, stimulated by the recent progress in our understanding of the distribution of galaxies in space derived from studies of the two-point correlation function and the early redshift surveys [e.g. (81) and other

work described in Section 1.3], to redetermine this space distribution. Their data immediately suggested that the galaxy distribution might be significantly smoother in the south Galactic polar cap ($b \leq -40°$) than in the north Galactic polar cap ($b \geq 40°$), and the correlation function that they derived was inconsistent with results from previous studies of the surface distribution of large samples of galaxies (104). This was sufficient to motivate Kirshner et al. (105) to obtain similar data for six representative fields $\simeq 1.4°$ on a side, three in the northern and three in the southern Galactic hemisphere, located near six of the fields in the previous survey but penetrating to the pioneering apparent magnitude limit $m_p \sim 17.5$ (corresponding to $V_{lim} \sim 30{,}000$ km $s^{-1} \simeq 0.1c$). The three northern fields are located approximately 35° equidistant apart on the sky near the periphery of the constellation Boötes, as illustrated in Figure 5.

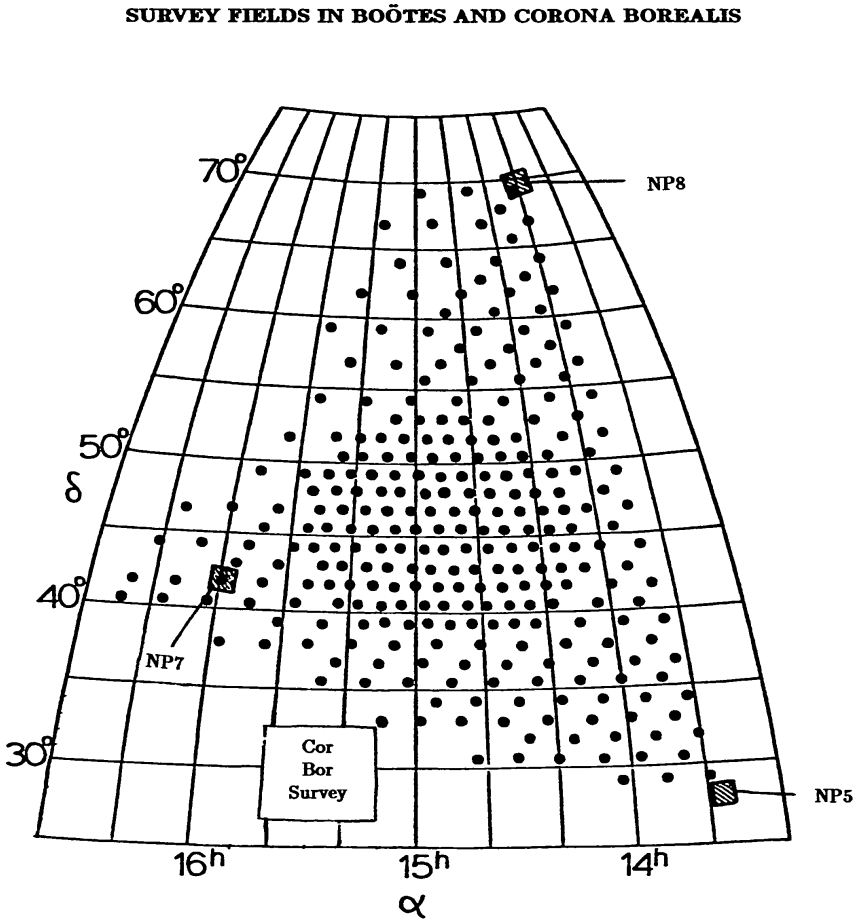

Figure 5 Location on the sky of (*a*) the original Boötes survey fields NP5, NP7, and NP8 of Kirshner et al. (105), (*b*) the 283 small square survey fields (represented by small circles) in the recent, more detailed survey of Boötes (106), and (*c*) the Corona Borealis survey field of Postman et al. (148a). Reproduced from (148a) by permission of M. Postman.

Kirshner et al. found that the histogram of observed redshifts for 133 galaxies in these three northern fields (90% complete redshift survey) is nearly empty in the interval between 12,000 km s^{-1} and 18,000 km s^{-1} (Figure 6*a*); this surprising result led them to make the plausible inference that the region within Boötes may contain a very large void (characteristic length ~ 120 Mpc) (105). To test this inference, they decided to survey the entire Boötes region in a representative manner to an apparent magnitude

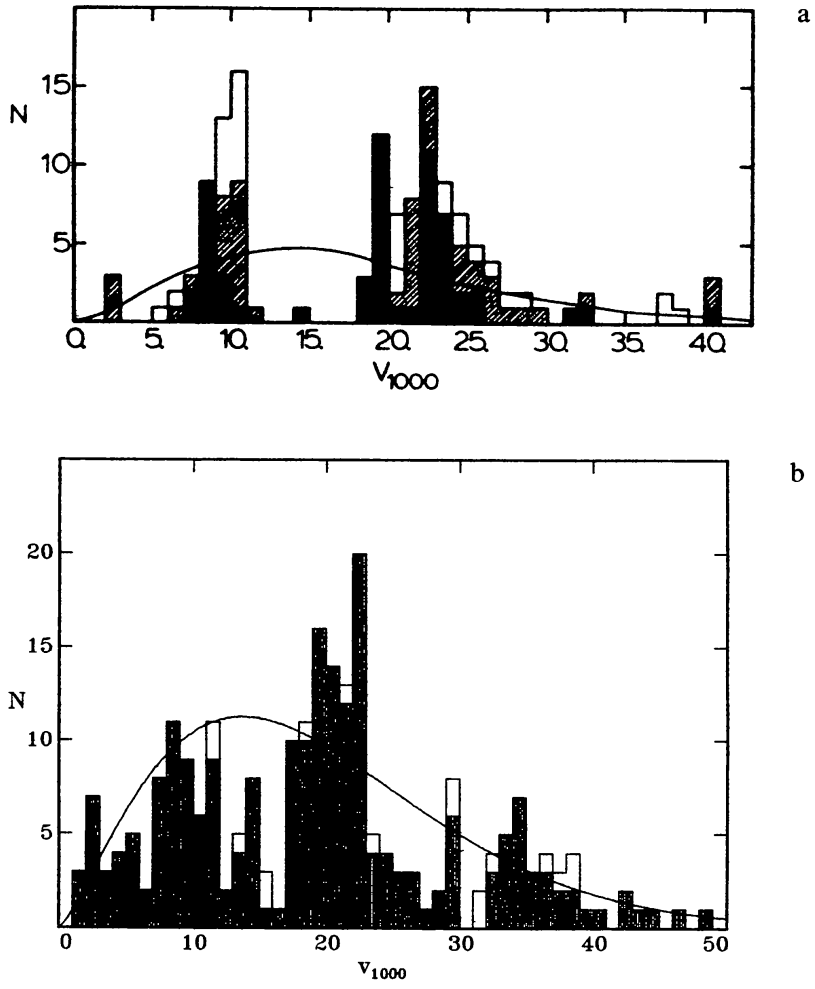

Figure 6 (*a*) Histogram of Doppler velocities in 1000 km s^{-1} intervals for a sample of 133 galaxies $\sim 90\%$ complete to $m_p \simeq 17.8$ in the 1.4 sq deg fields NP5 (dark), NP7 (light), and NP8 (hatched) depicted in Figure 5. The smooth curve is the distribution expected in a homogeneous universe. Reproduced from (105) by permission of R. P. Kirshner. (*b*) Corresponding histogram for a sample of 231 galaxies comprising (i) a subset $\sim 97\%$ complete to $m_p \simeq 17.5$ (dark shading) and (ii) other galaxies in 239 square fields 15′ on a side (out of the 283 small fields depicted in Figure 5). The smooth curve is the distribution expected in a homogeneous universe. Reproduced by courtesy of A. Oemler.

limit $m_p \sim 17.5$, measuring both redshifts and magnitudes for a large homogeneous sample of galaxies. This was accomplished by first selecting 283 small square survey areas 15 arcmin on a side, covering 2% of the sky area of the Boötes region, and distributed as shown in Figure 5. Then for each of these fields they visually identified galaxies and ranked them according to apparent luminosity. Apparent magnitudes of the galaxies were then estimated from these ranks (typically, for a given galaxy, the adopted rank is a logarithmic average of four values, one measurement per observer) calibrated by photoelectric magnitudes measured for 59 of the galaxies. Finally, redshifts were measured for 231 galaxies in 239 of the 283 survey fields (90% complete redshift survey to $m_p \sim 17.5$ in the subset of 239 fields). The resulting histogram is shown in Figure 6*b*. The region between 12,000 km s^{-1} and 18,000 km s^{-1}, while not empty, remains significantly deficient in galaxies relative to the number expected if the galaxies were homogeneously distributed in space. Moreover, the largest empty sphere that Kirshner et al. could place in the effective volume occupied by their sample has a radius $\simeq 60$ Mpc and is centered at $\alpha = 14^h50^m$, $\delta = 46°$, and Doppler velocity $V = 15{,}500$ km s^{-1}. Kirshner et al. point out that, curiously, this empty sphere does not extend as far as the three survey fields (NP 5, NP 7, or NP 8) on the basis of which the original discovery of the Boötes void was made. Kirshner et al. suggest that the most plausible explanation is that the void, although apparently sharply bounded in front and back, is surrounded in other directions by a larger region of low density that fields NP 5, NP 7, and NP 8 happen to penetrate at particularly empty spots (106). A direct test of this hypothesis requires an even more extensive redshift survey. [Additional review of work on the Boötes void is provided by Oort (128, p. 417) and Oemler (126b).]

The catalog by Zwicky et al. (220), constructed primarily by visual techniques, provides coordinates and magnitudes for the galaxies north of declination $\delta \simeq -3°$ complete to a limiting apparent magnitude $m_p \simeq 15.5$. This information is prerequisite for the CfA redshift surveys to (*a*) $m_p \leq 14.5$ and (*b*) $m_p \leq 15.5$. To construct deeper redshift surveys, and to study in more detail the structure of the Boötes void, it seems advisable to first create an analog of the Zwicky et al. (220) catalog, but to a limiting apparent magnitude of, say, $m_p = 17.5$ and by vastly more automated procedures. This goal is now within practical reach through the application of an automated plate scanner. One that is extremely fast, accurate, and in refinement-developmental stages is the automated plate scanner (APS) at the University of Minnesota; astronomers there are planning to use this instrument to create useful primary data bases of this type. The APS was initially built under the direction of W. J. Luyten specifically to carry out

a stellar proper motion survey, but it has been refurbished with new detection electronics and data-taking and processing equipment that make it a practical instrument to apply to a plate copy of the Palomar Observatory Sky Survey to construct an all-sky catalog of locations, magnitudes, and other properties of galaxies nearly complete to $m_p = 17.5$ (61, 96). The APS can automatically identify and measure all objects with $m_p \leq 17.5$ registered on a 14-inch × 14-inch plate of the Palomar Observatory Sky Survey in a scan time of $\leq 2^h45^m$ plus an equal reduction time. Completely automatic discrimination between stars and galaxies is achieved for most of the objects, and a semiautomated procedure achieves excellent discrimination for nearly all of the remaining objects. It appears that the APS system now provides a state-of-the-art technique for constructing the next-generation galaxy catalog of coordinates and apparent magnitudes, data that constitute a crucial prerequisite for next-generation galaxy redshift surveys.

It should be recognized, however, that the advanced technology (e.g. laser-beam scanning, computer and supercomputer reduction methods) represented by APS cannot now make morphological classifications of galaxies (61), so visual inspection of galaxies on photographic plates is still needed to construct catalogs with extensive, detailed, and *internally consistent* morphological information on galaxies (59b, 123a, 167a, 188b).

2.1.2 MATERIAL CONTENT OF VOIDS A recent review by Oemler (126b) contains information in addition to that provided below.

The following evidence supports the hypothesis that the Coma and Hercules voids are actually empty of matter: (*a*) Bothun et al. (30) studied the 4624 galaxies with known redshifts listed in the Nilson UGC catalog (123a). The sky was subdivided into cells of width 10° in declination and length 4^h. For each of these cells, a histogram of Doppler velocity for galaxies within each of three surface brightness categories was constructed. The three velocity histograms had similar shapes. More specifically, there was no tendency for redshift voids to be filled in by low-surface-brightness galaxies (see Section 3.1.2 for additional statistical evidence). (*b*) Thuan et al. (193) obtained a nearly complete sample of redshifts for 58 low-surface-brightness galaxies (the majority with $m_p > 15.5$) that are classified as dwarf, irregular, or Magellanic irregular in the UGC and that are located in the region of the sky for which the CfA redshift survey of galaxies with $m_p \leq 15.5$ is complete (Figure 4*a*). Thuan et al. found that the low-surface-brightness dwarf galaxies lie on the structures delineated by the normal high-surface-brightness galaxies. They do not fill in the voids. (*c*) The Coma void is evident in the three-dimensional distribution of IRAS infrared galaxies (A. Yahil, private communication, 1987). (*d*)

With the Green Bank 300-ft telescope, Krumm & Brosch (109) searched for neutral hydrogen clouds in roughly 7% of the Perseus-Pisces void and 19% of the Hercules void. No clouds were detected, and the detection threshold was sufficient for Krumm & Brosch to conclude that voids do not contain a cosmologically significant population of H I protogalaxies. Independent confirmation of this result, at about three times lower sensitivity, was recently obtained from observations with the Dwingeloo telescope by Hulsbosch (94a). Some *suspected signals* worthy of follow-up checks were identified in the latter study.

Although measured redshifts of the 22 surveyed IRAS galaxies within a region covering one-sixth of the solid angle of the Boötes void indicate that not one lies within the void (206a), the following results indicate that the Boötes void is not empty. (*a*) Superseding anticipatory results of Balzano & Weedman (20), Moody et al. (120a) discovered several emission-line galaxies (which typically, but not always, spectroscopically resemble H II regions with narrow lines and moderately weak stellar continua) in the Boötes void, bringing the total number of known emission-line galaxies in this void to eight. (*b*) Brosch & Gondhalekar (32) report the detection of absorption lines in the ultraviolet spectra of background quasars at the redshifts of the voids in Boötes and Perseus-Pisces; they state that the detection of metal lines suggests chemical enrichment of gas in the voids in support of the explosion-dominated model of formation of galaxies (98, 133). Additional discussions and interpretations of these observations are found in (33, 35, 136–138).

2.1.3 STRUCTURE OF CONTIGUOUS SHELLS The structure of superclusters, the material entities that make up the contiguous shells, is reviewed by Oort (128). Particularly interesting are correlations of structural properties of galaxies such as Hubble morphological type with local number density of galaxies, first discovered by Dressler (cf. 63a) for rich clusters and later found to extend monotonically into the domain of the dispersed component of superclusters (41, 84b).

The determination of the geometry of contiguous shells is basically a problem in map making [cf. Robinson & Sale (150) and MacKay (114)]. Ellis et al. (67) review the theoretical foundations of established astronomical methods for determining the structure of the Universe from telescopic observations. They also discuss selection effects introduced by this process. Barrow & Bhavsar (22a) examine factors that determine pattern recognition by the human eye, with special application to their role in the evaluation of whether large-scale structure is, for example, filamentary or cellular.

The geometry of contiguous shells derived by identifying observed Dop-

pler velocities of galaxies with their Hubble velocities is systematically distorted through the neglect of corrections for motions relative to the Hubble flow. The latter include (*a*) the motion of a galaxy in a system relative to the barycentric velocity of the system and (*b*) the motion of the system relative to the Hubble flow. Galaxies in clusters for which item (*a*) may cause significant distortions are generally excluded from analyses of geometrical structure. Although our knowledge concerning motions of systems of galaxies relative to the Hubble flow is still in an early state (Section 2.1.4), what we do know indicates that their effects can be neglected in estimating at least some broad features in the large-scale geometry of contiguous shells (42, 56, 57). Nevertheless, in detailed analyses, Fujimoto (79) and Kaiser (100b) demonstrated with several specific examples that the neglect of effects of peculiar motions relative to the Hubble flow can introduce some major geometrical distortions; for example, the infall motion caused by the self-gravity of a supercluster translates into a significantly sharpened contiguous shell, as estimated from uncorrected maps in velocity space (see Figure 4*a*).

2.1.4 KINEMATICS OF CONTIGUOUS SHELLS Previous reviews include Davis & Peebles (54) on evidence for local anisotropy of the Hubble flow, Mould (121) on the motion of the Local Group relative to the nearest clusters of galaxies, and Andersen (6) on recent indications of general streaming of galaxies within 100 Mpc.

Studies of galaxy samples within the Local Supercluster demonstrate that (*a*) the distance from the observed redshift by means of the Hubble relation and (*b*) the distance derived by a direct method that applies specific *intrinsic* structural properties of galaxies (e.g. the Tully-Fisher relation between H I velocity width and absolute luminosity of spiral galaxies, the Faber-Jackson relation between nuclear velocity dispersion and absolute luminosity of elliptical galaxies, and the approximately constant absolute luminosity of Sc I galaxies) display different systematic variations across the sky consistent with an infall velocity $\simeq 300$ km s^{-1} of the Local Group toward the Virgo cluster (54).

Similar studies of samples of Sc and elliptical galaxies beyond the Local Supercluster and within a volume of radius $\simeq 100$ Mpc have led to the detection (in the frame defined by the galaxy sample) of a velocity component of the Local Group in addition to infall velocity (cf. 2, 6, 50a, 113b, and references therein). But the derived values are very uncertain, and systematic effects may be insufficiently understood. Therefore, the relation of this motion to that derived from the anisotropy of the 2.75-K cosmic microwave background is currently unclear. The 0.1% cosine dependence (on sky angle) of the cosmic blackbody radiation is most simply interpreted

to indicate that our galaxy (also the Local Group) is moving (in the universal frame defined by the cosmic blackbody radiation) at a velocity of 600 ± 50 km s^{-1} toward a point in the constellation Hydra (212a). A recent study of an ensemble of galaxy clusters with distances between 80 and 200 Mpc indicates that the motion of the Local Group is within 250 km s^{-1} of that inferred from this microwave dipole anisotropy (1a, 121). Evidently, the velocity of the Local Group (in the universal frame defined by the cosmic blackbody radiation) contains a component in addition to its infall velocity (i.e. the component caused by the gravitational attraction of the Local Supercluster). This additional component may represent motion of the entire Local Supercluster. On the other hand, A. Yahil (private communication, 1987) reports that results from a study of the three-dimensional distribution of IRAS infrared galaxies (which are detectable into the obscuring layer of the Milky Way) indicate that the additional component represents transverse motion of the Local Group within the Local Supercluster or its very near proximity.

The detected infall velocity of the Local Group suggests that superclusters, i.e. the components of contiguous shells, expand internally at rates that are slower than the rate of universal expansion. It follows that the observed velocity of a local region on the perimeter of a void relative to its center (i.e. the velocity caused by its origin and dynamical evolution) contains (*a*) a positive component corresponding to the infall of galaxies within a supercluster and (*b*) an additional component corresponding to the cause of the difference between the 600 km s^{-1} velocity relative to the microwave background and the infall velocity of the Local Group. An outward velocity component of a void perimeter of ~ 500 km s^{-1} corresponds to a change in its characteristic length of ~ 20 Mpc in a Hubble time $\sim H_0^{-1}$.

2.2 *Indications From Distant Objects*

The galaxy redshift surveys described in Section 2.1 extend to $z \sim 0.1$, Abell rich clusters of distance classes $D \leq 4$ extend to $z \sim 0.1$, the more distant Abell clusters extend to $z \sim 0.3$, quasars extend to $z \sim 4$, and the cosmic blackbody radiation is believed to have originated at $z \sim 1000$. These tracers with different limiting effective redshifts facilitate comparison of present large-scale structure with that at epochs extending into the past up to the epoch of hydrogen recombination following the primordial fireball (48, p. 371).

2.2.1 ABELL CLUSTERS Previous reviews of this topic include Bahcall (11, 13) and Oort (128, pp. 403–8, 417–18).

In 1961, Abell (5) detected superclusters by visual inspection of the

surface distribution of rich clusters of galaxies listed in his catalog (4). A rudimentary 1976 study of superclustering among Abell clusters (154, 155) [which examined, for example, the three-dimensional spatial configuration of the 27 Abell clusters of distance classes $D \leq 2$ (complete sample) with known redshifts from Peterson (146)] was superseded by a parallel, but more extensive and more technically sophisticated 1982–86 analysis by N. Bahcall, R. Soneira, and W. Burgett [which examined, for example, the locational properties of the 104 Abell clusters of distance classes $D \leq 4$ (statistical sample) with redshifts from Hoessel et al. (90a)]. The Bahcall et al. study confirms the existence of superclusters of Abell clusters and provides a list of their membership (18). [Locations and other properties of the superclusters in the Northern Hemisphere are illustrated in Figure 21 of Oort (128, p. 406); similar but not identical memberships are depicted by the complete-linkage dendrogram, an especially informative branching diagrammatic representation of locational interrelations of Abell clusters (cf. 158 and Figure 7).] The Bahcall et al. study demonstrates that the correlation scale length (cf. Section 3.1.2) of the two-point correlation function of Abell clusters is ~ 50 Mpc, i.e. five times larger than that for galaxies (17) [cf. (65, 148) for evidence from independent observational studies that directly supports this result, and cf. (12, 25, 50, 100) for studies that explain the result astrophysically]. Furthermore, the study shows that if the separation vectors of cluster pairs in superclusters are derived by assuming that observed redshifts can be converted directly into distances through the Hubble relation, then the average radial (i.e. line-of-sight) component of the centroid of a pair, $\langle R \rangle$, tends to be larger than the average transverse component, $\langle T \rangle$ (19). This result is illustrated in Figure 8 with reference to the dendrogram superclusters depicted in Figure 7, and it is most naturally understandable as an effect of a characteristic non-Hubble relative velocity of clusters within superclusters, $\Delta V \sim 2000$ km s^{-1}. This value significantly exceeds the 600 km s^{-1} motion of the Local Group indicated by the anisotropy of the 2.75-K cosmic blackbody radiation and causes serious problems for various cosmological models advanced to explain large-scale structure (cf. Section 3.2.2); therefore, explanations in terms of observational uncertainties and elongation of large-scale structures are also being scrutinized in extensive detail (19). Finally, the Bahcall et al. study demonstrates that superclusters lie on the periphery of the Boötes void (16) [e.g. the Hercules supercluster lies on the near side and the Corona Borealis supercluster lies on the far side (the reader is referred to Figures 4, 5, and 6 for general locational orientation)]; that a void may be present in the three-dimensional distribution of Abell clusters, which extends from $l^{II} \simeq 140°$ to 240°, $b^{II} \simeq 30°$ to 50°, $z \simeq 0.03$ to 0.08, and has a characteristic length of ~ 300 Mpc (15); and that the

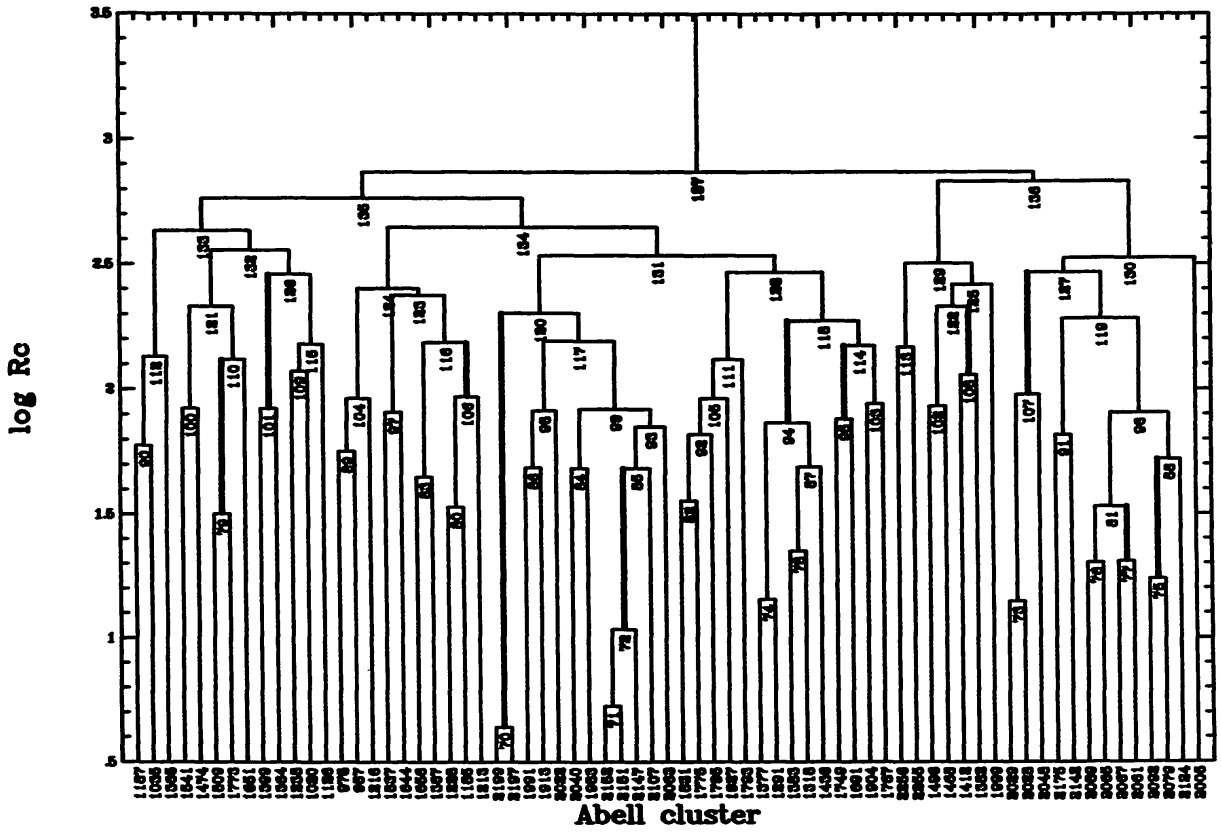

Figure 7 A complete-linkage dendrogram for the statistical sample of Abell clusters with distance classes $D \leq 4$ in the northern Galactic hemisphere (cf. 158). The ordinate specifies the similarity level [defined as the logarithm (base 10) of the complete-linkage distance] of a dendrogram supercluster, and the abscissa specifies the Abell designations (4) of its member clusters. Each dendrogram supercluster is represented by a hoop with a similarity bar, below which is written its identification number. (The superclusters Coma/A1367, Hercules/A2199, and Corona Borealis are Nos. 83, 120, and 86, respectively.) The similarity level of this bar represents the diameter of the dendrogram supercluster. The vertical line that extends upward from the center of the bar of the dendrogram supercluster is one of the two branches of the hoop representing the next higher dendrogram supercluster in its membership hierarchy (its neighborhood supercluster). A darkened branch means that the *dendrogram* supercluster is a *physical* supercluster modulo $\delta_L > 20$, where δ_L is the local density contrast, i.e. the number density of the dendrogram supercluster divided by the number density of the neighborhood supercluster.

superclusters may be correlated on a scale of $\sim$200 Mpc, suggesting the possible existence of the largest structures yet detected (14).

Batuski & Burns (24) and Burns & Batuski (33b) adopt a different approach to the study of large-scale structure with data for Abell clusters. Instead of concentrating on the Abell clusters of the statistical sample with measured redshifts, they apply data for all 2712 Abell clusters (statistical plus nonstatistical sample) with measured plus estimated redshifts. This causes a loss of homogeneity and accuracy in the data base, which,

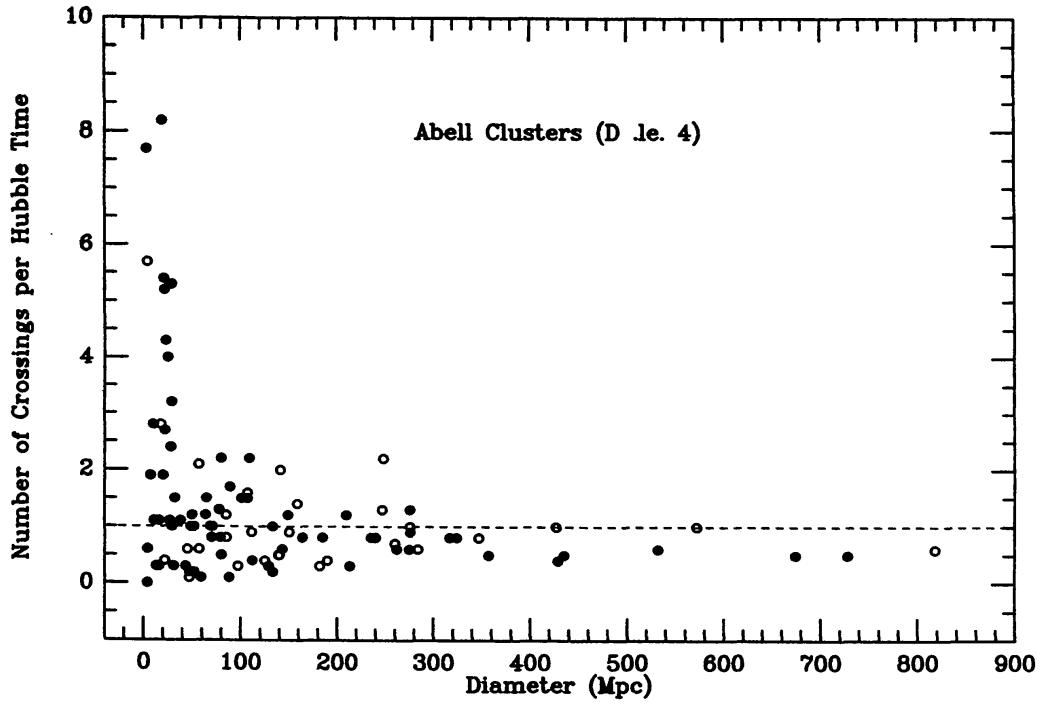

Figure 8 The ordinate represents $N_{\text{crossings}}$, the number of crossing distances traversed by a cluster in its dendrogram supercluster over one Hubble time-scale (H_0^{-1}). Superclusters in the northern and southern Galactic hemisphere are represented by closed and open circles, respectively. The crossing distance is defined as the radius of a dendrogram supercluster. $N_{\text{crossings}}$ is estimated from the formula $N_{\text{crossings}} = \sqrt{2}\sigma_R/\sigma_T$, where the separation vectors of the R_{ij}-pairs of clusters in a supercluster are estimated from the angular separations and the Hubble distances of the clusters (cz/H_0), σ_R is the standard deviation of the radial (i.e. line-of-sight) component of the separation vectors relative to the average for the system, and σ_T is the corresponding standard deviation of the transverse (i.e. in the plane of the sky) component. The abscissa represents D_c, the diameter of a dendrogram supercluster (estimated to be its complete-linkage distance). An interesting exercise for the reader is to identify the selection effect that causes the calculated $N_{\text{crossings}}$ to approach 0 as D_c approaches the effective limiting diameter of the volume containing the sample of Abell clusters. This figure illustrates (in a different way) the redshift broadening that could indicate the relative velocities of Abell clusters in superclusters of $\sim$2000 km s^{-1} discovered by Bahcall et al. (19).

however, is counterbalanced by an increase in the number of tracers that characterize the large-scale structure. Each assigned redshift has been either measured directly or *estimated* through a calibration curve from the apparent red magnitude of the tenth most luminous cluster galaxy measured by Abell (4). Because the fractional uncertainty of an estimated redshift is $\sigma_z/z \simeq 0.3$, the increased sample with estimated redshifts typically causes a decrease of the ratio of signal to noise (S/N) for the identification and delineation of structures, but for *very large* structures, S/N *increases*. From the rough three-dimensional distribution of the 652 Abell clusters with measured or estimated redshifts $z \leq 0.13$, Batuski & Burns

(24) constructed a finding list of 102 candidate superclusters and 29 candidate voids with measured or estimated redshifts less than $z \simeq 0.1$. They identified the candidate superclusters as the islands created by the linking of overlapping spheres of sweeping radius $R_s = 60$ Mpc attached to each Abell cluster.[1] The four candidate superclusters with the largest membership of Abell clusters and with more than 50% of their redshifts measured are illustrated in Figure 9. Batuski & Burns (23) found that the Pisces-Cetus supercluster (A in Figure 9) located near the southern Galactic cap is part of a possible filament of galaxies and galaxy clusters with a characteristic length ~ 450 Mpc. In an independent investigation (204, 204a), Tully pointed out that if the supercluster-identifying sweeping radius in the Batuski & Burns sample of Abell clusters is increased by only 50% to $R_s = 90$ Mpc, then a dramatic change occurs in which the Pisces-Cetus supercluster links with both the Coma/A1367 supercluster and the Local Supercluster. (The linked structure is a band containing ~ 60 rich clusters that stretches across the entire sky through both the southern and northern Galactic caps!) Moreover, the main plane of this Pisces-Cetus supercluster complex (characteristic length ~ 500 Mpc and thickness ~ 60 Mpc) is coincident with the principal plane of the Local Supercluster [characteristic length ~ 50 Mpc and thickness ~ 8 Mpc; cf. (203), (204), and Oort (128, pp. 380–84)], which suggests that the two structures are physically connected. M. Postman, D. Spergel, & B. Sutin (private communication, 1987) are comparing the observational data with corresponding data generated from computer simulations of models that incorporate selection functions derived from the observational data; the results of these comparisons could provide quantitative estimates of the statistical significance of Tully's observational results. A historical precedent for these kinds of studies on the Pisces-Cetus supercluster complex is found in earlier published studies on the Local Supercluster itself (cf. 9, 58, 59).

Although a definitive answer concerning the physical existence of the Pisces-Cetus supercluster complex must await results of quantitative simulation analyses such as that by M. Postman et al. and observational analyses with measured redshifts for the complete sample of Abell clusters with $z \leq 0.13$, I suggest that the hypothesis of a physically real Pisces-Cetus

[1] This "percolation technique," introduced in another context by Turner & Gott (205a) and later introduced to the study of superclustering by Zel'dovich et al. (216), is discussed more fully by Oort (128, pp. 409–11), and is one of a family of related supercluster identification techniques (Section 3.1.3). A given sweeping radius applied to a sample of clusters that is selection-free (or for which selection effects have been removed) specifies a given minimum local number density for supercluster membership, $\rho_{min} = (4\pi R_s^3/3)^{-3}$, which corresponds to a minimum global density contrast δ_G; for example, Bahcall & Soneira (18) identified 16 superclusters with $\delta_G \geq 20$.

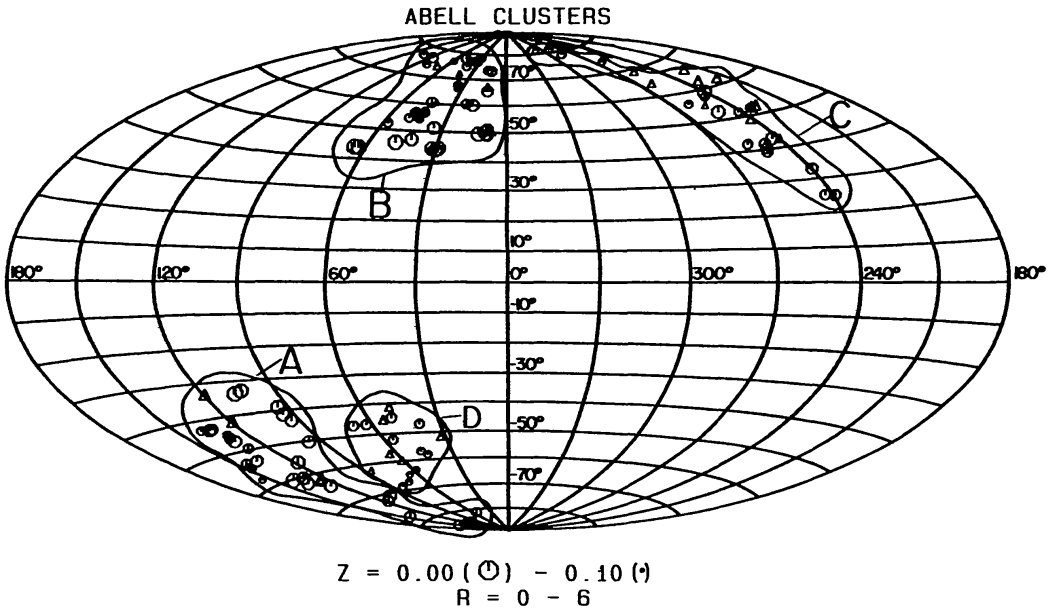

Figure 9 Aitoff equal-area projection of the celestial sphere in Galactic latitude (b^{II}) and longitude (l^{II}) displaying the locations of the Abell clusters in all richness classes ($R = 0$–6) contained in four of the supercluster candidates of Batuski & Burns (24). Octagons and triangles signify clusters with measured redshifts and estimated redshifts, respectively. The legend contains the limits of the sizing scheme for the symbols (linear in redshift). The four candidates, outlined by contour lines, are (A) Pisces-Cetus, (B) Sextans-Leo, (C) extended Hercules, and (D) Aquarius. By inspecting the chart representing the sky distribution of Abell clusters reproduced in Figure 20 of Oort (128, p. 404), we note that the zone of Galactic obscuration lies between $b^{II} \simeq -30°$ and $b^{II} \simeq 30°$ and that the southern equatorial hemisphere, which (for practical reasons) is not part of the Palomar Observatory Sky Survey, lies primarily in the lower right-hand quadrant of the plot. The region occupied by the Pisces-Cetus supercluster complex, with its characteristic length ~ 500 Mpc studied by Tully (204), extends from the elongated Pisces-Cetus supercluster (A) through the Galactic plane at $l^{II} \sim 120°$ and the Coma cluster near the northern Galactic pole. The Local Supercluster (centered near $l^{II} = 284°$, $b^{II} = 74°$) is contained within this supercluster complex. The void of Abell clusters, with its characteristic length ~ 300 Mpc identified by Bahcall & Soneira (15), extends from $l^{II} \simeq 140°$ to 240°, $b^{II} \simeq 30°$ to 50°, and redshift $z \simeq 0.03$ to 0.08. Reproduced from (24) by permission of D. J. Batuski and J. O. Burns.

supercluster complex might make more understandable at least two astronomical puzzles: (*a*) The polar Galactic extinction derived from the classical interpretation of galaxy counts is much larger than the accepted value (0.2 mag) derived from less suspect methods (59b). The Pisces-Cetus supercluster complex would introduce a previously unrecognized bias that acts in the direction of the effect. The steep selection function in Galactic latitude that has been derived from the surface distribution of Abell clusters (17) (corresponding to an equivalent polar extinction of 0.5 mag) may also contain a component from this very large structure. The discovery by

Kirshner et al. (104) that the galaxy distribution is significantly smoother in a sampling of the south Galactic polar cap than in a sampling of the north Galactic polar cap may be related to the structure of the Pisces-Cetus supercluster complex. (*b*) The Local Group moves with a velocity of 600 km s^{-1} relative to the frame of the cosmic microwave background (212a), which is consistent (within the uncertainties of measurements of velocities and especially distances) with results from local samples of galaxies within an effective distance of $\sim$100 Mpc (2, 6, 50a, 113b). There is also an indication from studies of kinematic properties of elliptical galaxies within a distance of $\sim$100 Mpc that this entire local region might be participating in this motion (6, 113b). Bulk motion would be understandable if the Pisces-Cetus supercluster exists, and part or all of the 600 km s^{-1} motion of the Local Group relative to the frame of the microwave background could be caused by the gravitational attraction of this supercluster complex. [A local feature sometimes called the "Great Attractor," located at a distance of $\sim$90 Mpc positioned on the sky just below the Centaurus cluster (Figure 10), has previously been suggested to cause bulk streaming motion (6, 113b). Comparison of Figures 8 and 9 indicates that the "Great Attractor" is located on the great circle of the Pisces-Cetus supercluster complex and hence is likely to be a nearby part of this relatively planar structure.] The mass of the Pisces-Cetus supercluster complex is $M = 10^{17}$–$10^{18}\ M_\odot$, derived by Tully (204) from summing the mass expected to be associated with the number of Abell clusters in the complex (cf. 12, 45) and, alternatively, by estimating the fraction of mass in the volume occupied by the complex in a universe with a density parameter $0.1 < \Omega < 1$. The Local Group and the galaxies in its environs would be falling toward the center of the Pisces-Cetus supercluster complex with an infall velocity given by $\Delta V_{\rm in} = GM/R^2H_0$. For $R \sim 250$ Mpc and $M \sim 10^{17}$–$10^{18}\ M_\odot$, $\Delta V_{\rm in} \sim 150$–1500 km s^{-1}, consistent with the observed peculiar velocities relative to the Hubble flow (e.g. $\Delta V_{\rm in} = 600$ km s^{-1} corresponds to $M \simeq 4 \times 10^{17}\ M_\odot$).

The location of the $\sim$300 Mpc void identified by Bahcall & Soneira (15) (see above) is noted in the caption for Figure 9. From analysis of their extended sample of Abell clusters, Batuski & Burns (24) and D. J. Batuski et al. (private communication, 1987) find that this is indeed an extremely large region of very low cluster density; knowledge of whether or not it will break up into a collection of smaller voids, however, must await direct redshift measurements for the Abell clusters whose estimated redshifts would place them in or near this void.

2.2.2 QUASARS Previous reviews of this topic include Tanaka & Ikeuchi (190) and Oort (128, pp. 408–9).

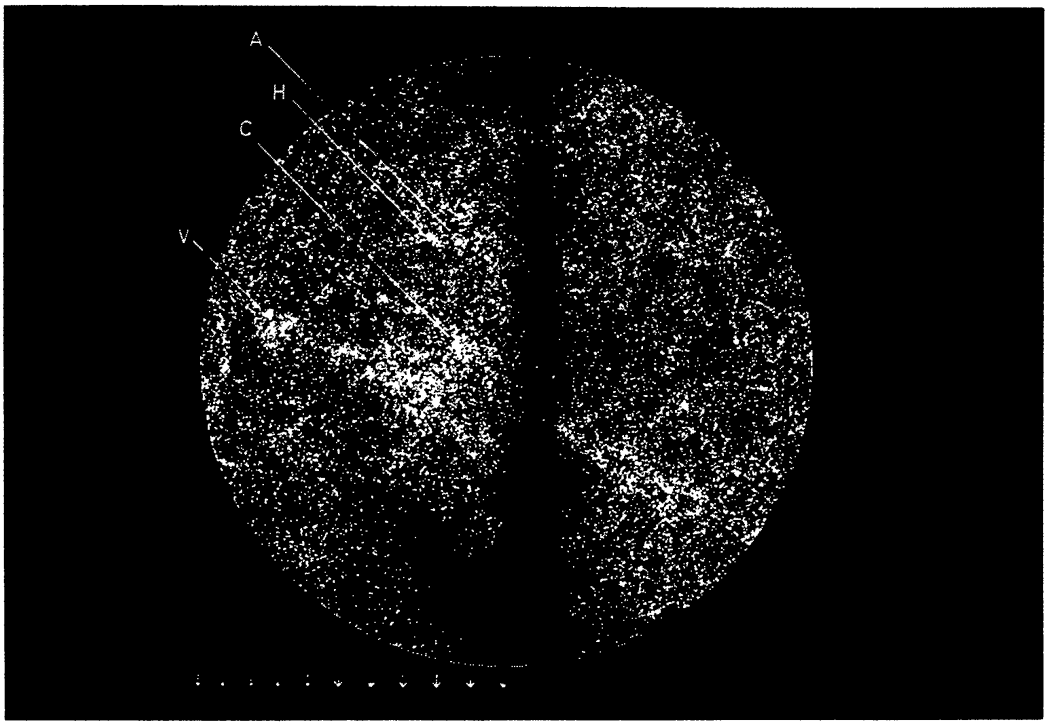

Figure 10 Computer-generated sky map by O. Lahav of galaxies with blue apparent magnitude smaller than $m_p \sim 14.5$. The plot is centered at $l^{II} = 307°$, $b^{II} = 9°$, the direction of streaming motion found from a sample of elliptical galaxies within a volume of radius $\simeq 100$ Mpc by Lynden-Bell et al. (113b). The dark vertical band represents the zone of avoidance caused by Galactic obscuration. The location of the Galactic center is 37° up from the bottom of the picture. The Virgo (V), Centaurus (C), Hydra (H), and Antilia (A) clusters are indicated. The "Great Attractor" is the great concentration of galaxies just below the Centaurus cluster. The nonlinear scale indicates 9° intervals spanning the range from the center to the edge of the picture. Reproduced from (113b) by permission of Sandra Faber and O. Lahav.

The distances of most quasars are much larger than the distances of galaxies and clusters of galaxies from which superclusters and voids have been detected in the large-scale structure. Shaver (180) discusses the possible existence of very large scale structure in the three-dimensional distribution of quasars, especially at redshifts $z \leq 0.5$. Oort (127, 129) suggests that the redshift separation between known superclusters evolved back to $z = 2.5$ is of the same order as the separation between the strongest Lα absorption systems observed in quasars (cf. 170a), which suggests that the absorption systems may be caused by uncondensed Zel'dovich pancake gas (215, 215b, and Section 1.3) that has remained uncondensed. Detailed analyses of physical constraints for the gaseous clouds that are the Lα absorbers have been derived by, for example, Melott (117) and Ostriker & Ikeuchi (134), who discuss alternative models.

2.2.3 COSMIC BLACKBODY RADIATION Previous reviews of this topic include Sunyaev & Zel'dovich (189) and Wilkinson (212a).

Evidently, the cosmic blackbody radiation was generated by primordial material with fluctuations in mass density that later evolved into the (superclusters + voids) large-scale structure that we observe today. Searches are in progress to detect a signature of these fluctuations in the form of irregularities in the sky distribution of the cosmic blackbody radiation. Wilkinson (212a) reports that the 0.1% cosine distribution of the all-sky cosmic blackbody radiation (interpreted to represent a 600 ± 50 km s^{-1} motion of the Local Group relative to the frame defined by this radiation) shows no ripples on smaller angular scales at 10% of that level. In particular, bumpiness with angular scales of about 10 arcmin has not yet been seen (cf. Section 3.2.2).

3. ENSEMBLES OF VOIDS (CURRENT STUDIES)

Previous reviews of topics discussed in Section 3 include de Lapparent et al. (57), Doroshkevich et al. (63), Fall (69a), Krauss (108), Peebles (144), Rees (148d), Shandarin & Zel'dovich (176), Silk et al. (182), Sunyaev & Zel'dovich (189), Waldrop (210b), White (211e), and Zel'dovich et al. (216).

3.1 *Statistical Representations of Void Data*

Once a homogeneous sample of superclusters or individual voids is identified, their structural properties can be determined and then studied statistically, just as is done for other cosmic objects (e.g. stars, supernova remnants, galaxies); in 1981, Oort (127) pointed the way. The locational properties of the galaxies or clusters that constitute the homogeneous data bases used to identify voids can also be studied by statistical methods to learn about void properties and their relation to predictions of models; the techniques and results are described below.

3.1.1 POISSON VOIDS (SUBTLETIES) Individual voids in the space distribution of *galaxies* with characteristic lengths of ~ 50 Mpc were first recognized definitively by visual inspection (Sections 1.3, 2.1.1); the Coma and Hercules voids are illustrated in Figure 4. Bahcall & Soneira (15) presented a variety of evidence that suggests the physical presence of a void in the space distribution of the 71 northern Abell *clusters of galaxies* (statistical sample, distance classes $D \leq 4$) corresponding to $N_t \simeq 52$ superclusters distributed according to the selection function $f(b) = 10^{0.3(1-\csc b)}$ (where b is Galactic latitude) in solid angle $\Omega_t \simeq \pi$. The void was detected visually as an empty region of solid angle $\Omega_v = g_v \Omega_t$ (where $g_v \simeq 1/7$) in

the surface distribution of Abell clusters. From an analysis of 100 computer model simulations and an analytical calculation for a model of N_t superclusters with uniformly Poisson-distributed locational coordinates, they estimated that the statistical probability for the chance occurrence of a void of solid angle $\Omega > \Omega_v$ is $P_v \leq 0.01$. Politzer & Preskill [147; see also (135)] proved that a void *search-procedure* correction must be applied to Bahcall & Soneira's analytical calculation [to allow for the fact that Bahcall & Soneira identified the void by scanning the survey area Ω_t to find the largest empty region, Ω_v, and not by placing search windows of solid angle Ω_v at random (or, alternatively, evenly spaced) locations within Ω_t]. Hence, Bahcall & Soneira's probability formula $P_v \simeq \Omega_t/\Omega_v \times e^{-N_t g_v}$ became replaced (for circular voids) by Politzer & Preskill's $P_v \simeq \Omega_t/\Omega_v \times (N_t g_v)^2 \times e^{-N_t g_v}/f_c$ (where f_c is a fiducial correction factor to exclude circles that overlap the boundary of the sample), so that $P_v \sim 0.2$. The value is even larger if the shape of the void is allowed additional degrees of freedom [see (147)]. The factor of >20 discrepancy between the value of P_v derived from computer model simulations and the value derived analytically is unexplained at this time.

3.1.2 STATISTICAL PROBABILITY TECHNIQUES To study voids by means of statistical probabilities, a statistic must first be identified that provides a well-defined signature for the presence of voids. Then the probability-density or distribution function of that parameter is calculated from the locational coordinates of the galaxies in the sample. Finally, a comparison is made between this observed probability function and the predicted probability functions calculated from mathematical and astrophysical models with the same number of galaxies and the same observational selection functions as in the observational sample to identify that model which provides the best fit to the observed probability function.

Early statistical studies of large-scale structure applied primarily the spatial two-point and occasionally n-point correlation functions (cf. 142, 142a, pp. 138–256; 198). Correlation functions are insensitive to void structure (cf. 77, 84, 114a), so the extensive work on determining correlation functions from observational data, while contributing to our general knowledge of large-scale structure, contributed not at all to the discovery of voids. One can think of the observed two-point correlation function, the structure indicator SI of R_{ij}, as a construction from the totality of the $N(N-1)/2$ separation vectors of length R_{ij} (where the N galaxies in the homogeneous sample are numbered from $i, j = 1$ to N). The two-point correlation function provides information on the observed large-scale structure relative to a (structureless) model with Poisson-distributed locational coordinates, and it is defined as $SI = [N(R_{ij})/$

$N(R_{ij})_{\text{Poisson}}]-1$, where $N(R_{ij})$ is the number of observed galaxy pairs with R_{ij} to $R_{ij}+\Delta R_{ij}$. Here ΔR_{ij} is a standard interval chosen to be sufficiently large so that SI is statistically well determined at the smallest R_{ij} of interest, but small compared with the effective radius of the cosmic volume containing the sample of N galaxies. $N(R_{ij})_{\text{Poisson}}$ is the corresponding number of pairs with R_{ij} to $R_{ij}+\Delta R_{ij}$ averaged over N_S samples (where $N_S \rightarrow \infty$), each sample with N galaxies constructed from an initially Poisson distribution of locational coordinates to which the observationally derived selection functions have been applied. The n-point correlation function is obtained by generalizing these concepts to encompass the joint distribution of the n separations: R_{ij}, R_{ik}, etc. The observed two-point correlation function is observationally well described by a power law, i.e. $SI = AR_{ij}^{x}$, where A is the correlation amplitude and x is the "slope." The correlation scale length R_L is the value of R_{ij} for which $SI = 1$, i.e. $R_L = A^{-1/x}$. Analysis of data on locational coordinates of galaxies and galaxy clusters indicates that $x \simeq -1.8$ for both types of cosmic object, but $R_L \simeq 10$ Mpc for galaxies and $R_L \simeq 50$ Mpc for galaxy clusters (cf. Section 2.2.1). Additional information on large-scale structure is contained within the values of corresponding parameters for the hierarchy of n-point correlation functions; for example, within this framework, Fry (78a) studied statistics to quantify the visual impression of filaments in galaxy maps.

White (211c) derived and displayed relations that can be used to express any quantitative measures of clustering in terms of the hierarchy of correlation functions. He found that on scales less than the expected nearest neighbor distance most measures are influenced only by the lowest order correlation functions, and on all larger scales the measures depend significantly on higher order correlations only. White then suggested a particularly appealing statistical probability function that is influenced by correlation of all orders: the probability density function $p(r)$, or, alternatively, the distribution function, $g(r) = \int_r^\infty p(r)\,dr$, of the distance r from a randomly chosen point to its nearest galaxy neighbor; $p(r)$ and $g(r)$ are very sensitive to the presence of voids (cf. 3). For a Poisson reference model of galaxies with randomly distributed locational coordinates [i.e. the local number densities $n(x, y, z)$ equal the global number density n to within Poisson uncertainties], we have $g(r) = e^{-nr}$. The probability functions $p(r)$ and $g(r)$, and other closely related probability functions, seem to encompass the entire set of probability density and distribution functions that have been used to study the nature of voids as indicated by the locational properties of homogeneous samples of galaxies. Void-sensitive probability functions of this type have been derived for many mathematical and astrophysical models (cf. 3, 78, 84, 171); as demonstrated by Fry (78), for example, the main advantage of this type of analysis is that evolution

and other effects are reduced to a single statistic whose distribution is model sensitive. Some of these mathematical and astrophysical models have been subjected to the selection functions derived from observational data of homogeneous samples of cosmic objects, and the resulting predicted probability functions have been compared with the corresponding empirical probability function derived directly from the observational data (cf. 31, 140, 167, 186, 208, 209). Probability functions derived from observational samples of galaxies with different ranges of absolute luminosity are consistent with the assumption that the less luminous galaxies do not fill in the voids (167, 186; see also Section 2.1.2). Finally, I note that the above statistical procedures to study voids, which have been applied extensively to samples of galaxies, seem not to have been applied to samples of Abell clusters of galaxies. This may be a consequence of a reluctance to accept the homogeneity of the statistical sample of Abell clusters (which was identified visually). Abell (4) documents the care taken to insure that the sample is statistically homogeneous so that it can be used for statistical studies [with the proviso that care must be exercised to allow for effects of the random and systematic uncertainties of the data, as has been done in the work by, e.g., N. Bahcall et al. (Section 2.2.1)]. Concrete studies to settle this issue are in progress.

Void-sensitive probability functions such as $p(r)$ and $g(r)$ derived from observational galaxy data have been related to the amplitudes of the n-point correlation functions by Sharp (179) [from data in the Zwicky catalogue (220)] and by Bouchet & Lachiéze-Rey (31) [from data in the CfA catalog (93a)]. Masson (114a) points out that correlation function analysis cannot distinguish between overdensity and underdensity structure. Fry (77) and Hamilton (84) show that the qualitative and to some degree quantitative aspects of $n(x, y, z) \ll n$, the spatial density function at the small local densities appropriate to voids that is recovered from the amplitudes of the n-point correlation functions, is largely independent of the exact sequence of amplitudes [i.e. the correlation amplitudes provide a poor characterization of $n(x, y, z)$ within voids].

3.1.3 DENDROGRAM ANALYSIS All the information on large-scale structure extractable from a homogeneous sample of N cosmic objects is contained in the $N(N-1)/2$ separation vectors of length R_{ij}. The two-point correlation function extracts from these data two parameters, a slope (x) and amplitude (A), and the n-point correlation functions contain $2n$ corresponding parameters. Correlation functions do not cleanly separate internal from global structural properties of systems of objects. Complete-linkage dendrograms, which use only those R_{ij}'s that refer to global structure, were introduced to astronomy by Materne (115).

A complete-linkage dendrogram (e.g. Figure 7) diagrams the results of an abstract elimination tournament. A sphere with sweeping radius R_s [cf. Section 2.2.1 and Oort (128, pp. 409–11)] is centered on each object. The x-axis of the dendrogram contains N evenly spaced *nodes*, one for each object. As R_s increases, the spheres begin to overlap. The first contact of two expanding spheres is represented by a *dendrogram hoop*, composed of two nodes, two vertical branches, and a horizontal *similarity bar*. The branches connect the nodes to the ends of the similarity bar. The midpoint of a similarity bar forms a new node. The y-coordinate of a similarity bar specifies the similarity level of the corresponding dendrogram system. The similarity level could be defined, for example, by the logarithm of R_c, the complete-linkage distance, i.e. the *largest* R_{ij} among the mutual separations of the M objects in the dendrogram system. (The single-linkage distance, i.e. the sweeping radius that resulted in the link, is the *smallest* R_{ij} among the mutual separations of the M objects in the dendrogram system.) R_c is an approximation to D_c, the major diameter of the dendrogram system.

A dendrogram contains information about both large-scale structure and individual structures. Parameters such as $\langle M \rangle$ and σ_M, the average multiplicity and rms multiplicity of the $(N-1)$ dendrogram systems comprising the N objects, are model sensitive. D_c and M, the diameter and multiplicity of a dendrogram system, are fundamental global properties of a system. Subsets of physical systems among the dendrogram systems can be readily extracted by adopting a criterion for physical reality based on, for example, global or local number density contrast or, similarly, overdensity (if physical superclusters are to be identified) or underdensity (if physical voids are to be identified). For an observational sample and mathematical/physical models with the same number of objects and same selection functions, one can construct (by analogy with the definition of the two-point correlation function) the function SI of D_c, defined as $SI = [N(D_c)/N(D_c)_{\text{Poisson}}] - 1$, which compares (for the sample of interest) the distribution of characteristic lengths of the observed dendrogram systems with that for a Poisson sample with the same number of objects and the same selection functions. Or one may wish to calculate an especially void-sensitive function, e.g. SI of D_v (where D_v is the characteristic length of a void), derived from the dendrogram systems with left and right nodes (L and R) each located on either the x-axis [characteristic lengths $D_c(\text{L}) = 0$ and $D_c(\text{R}) = 0$] or the similarity bar of the hoop representing a previously identified dendrogram system (nonzero characteristic lengths). An estimate of D_v is provided, for example, by $D_v = D_c - [D_c(\text{L}) + D_c(\text{R})]$. The wealth of research possibilities of dendrograms in general, and complete-linkage dendrograms in particular, toward identifying physical systems in astron-

omy and clearly describing basic properties of large-scale structure has only begun to be tapped (115, 158, 191, 201a, and references therein).

Complete-linkage dendrogram analysis is one of a family of broadly related techniques. Oort (128, pp. 409–11) reviews (*a*) "percolation cluster analysis," which analyzes plots of the complete-linkage distance vs. the single-linkage distance, and (*b*) "multiplicity function analysis," which analyzes the frequency distribution of multiplicities of dendrogram systems. Bhavsar & Barrow (27) recently did a percolation cluster analysis on the CfA (93a) sample of galaxies and a corresponding sample generated by *N*-body simulations of gravitational clustering (2a). Dekel & West (55) find that percolation is an insensitive discriminant between models of clustering that are very different. (The reader should be cautioned *not* to assume *a priori* that this result necessarily also applies to any other given technique based on the concept of a sweeping radius.) Interesting new techniques that for some purposes may provide complementary or preferred information to that accessible through study of complete-linkage diagrams include analyses with "minimal spanning trees" described by Barrow et al. (22b) and "taxonomical analysis" introduced to astronomy by Paturel (141a) and applied recently by Moles et al. (120; also 145, 145a).

3.1.4 POINT-SMOOTHING ANALYSIS Gott et al. (80) [also see (80a, 84a, 211), J. R. Gott III & A. L. Melott (preprint, 1986), D. Weinberg & A. L. Melott (preprint, 1986), and A. L. Melott, D. Weinberg & J. R. Gott III (preprint, 1987)] introduce at least three new ingredients into the analysis of three-dimensional large-scale structure: point smoothing, high-contrast mapping, and a *topological genus parameter* to distinguish between different models. The analysis is done with data from the CfA redshift survey complete to apparent magnitude $m_p \sim 14.5$. A "cosmic cube" with an effective edge length of ~ 140 Mpc was selected for which the census of galaxies with absolute magnitude $M_p \leq -20.5$ is complete. Each of the 153 galaxies in the cosmic cube is given a unit mass that is smoothed into a density distribution over a volume with an effective smoothing length $R_{es} \simeq 19$ Mpc selected to be sufficiently large so that distorting effects of motions of galaxies [cf. (100b) and Sections 2.1.3 and 2.1.4] are "small." At each location in the cosmic cube, the total local density is then calculated by summing the contributions from the smoothed individual galaxies. The known density distribution in the cosmic cube is then used to construct a high-contrast three-dimensional map that consists of "white" and "black" regions corresponding to local densities larger or smaller than the medium value, respectively. Thus, half of the volume of the cosmic cube is "white" and half is "black." If theoretical considerations are neglected, then the resulting topology of the cosmic cube is surprising. Instead of white polka

dots (individual superclusters) on a black background [model (*a*) in Section 1.1] or black polka dots (individual voids) on a white background [model (*b*) in Section 1.1], the white and black regions were found to be connected, equivalent, and completely interlocking, a connected white structure intertwined with a connected black structure (one supercluster, one void), a spongelike topology [model (*c*) in Section 1.1].

Gott and coworkers point out that for a large class of cosmological models [cf. Oort (128, pp. 418–25) and Section 3.2.2], spongelike topologies are physically consistent with having equivalent high- and low-density regions in the initial fluctuations. The topology does not change so long as the fluctuations are in the linear regime. The topology of the two-dimensional surface specified by the median density separating the black and white regions is characterized at a particular location by the Gaussian curvature $K = 1/a_1a_2$, where a_1 and a_2 are the principal radii of curvature at that point. For a large class of surfaces, the integral of the Gaussian curvature over the surface is given by the Gauss-Bonnet theorem, $I = \int K\,dA = 4\pi(1-g)$, where g is the genus of the surface. Loosely speaking, g is the number of holes contained in the surface: for a sphere, $g = 0$; for a donut, $g = 1$; for a sphere with N_h handles, $g = N_h$; and for two spheres, $g = -1$. In applications, Gott and collaborators calculate (*a*) the genus of the median density surface and other contours of the smoothed density distribution and (*b*) the mean genus per unit volume. Results derived for the galaxy distribution in the cosmic cube of the CfA sample are compared with corresponding results for models derived from numerical simulations of galaxy clustering (cf. Section 3.2.2).

3.2 *Theoretical Studies*

3.2.1 DYNAMICAL EVOLUTION OF VOIDS A typical void has a radius $R_v \sim 25$ Mpc and a sharp contiguous shell of superclusters with a non-Hubble velocity (assumed outward relative to the center of the void) $V_{vs} \sim 600$–1400 km s^{-1}. (The range is defined by the velocity of the Local Group relative to the cosmic microwave background and the relative velocity of Abell clusters in superclusters.) This velocity includes a component $V_{in} \sim 300$ km s^{-1} from infall of galaxies toward the center of a supercluster. To this reviewer, these observed parameter values seem nicely consistent with the results of the basic theoretical considerations now described.

We adopt a model consisting of a galaxy located in a group (or cluster), within a supercluster, constituting part of the contiguous shell of a void in a universal homogeneous background of matter. The velocity $\mathbf{V}_g$ and radius vector $\mathbf{R}_g$ of the galaxy are referred to an origin at the center of the void. The velocity of the galaxy is specified by the vector relation

$\mathbf{V}_g = \mathbf{V}_{vir} + \mathbf{V}_H + \mathbf{V}_{in} + \mathbf{V}_{out} + \mathbf{V}_{ex}$, where $\mathbf{V}_{vir}$ is the virial velocity relative to the barycenter of the group, $\mathbf{V}_H$ is the Hubble (cosmological) velocity corresponding to the universal background, $\mathbf{V}_{in}$ is the supercluster infall velocity [caused by the overdensity of the supercluster relative to the mass density of the universal background], $\mathbf{V}_{out}$ is the void outflow velocity (caused by the underdensity of the void relative to the mass density of the universal background), and $\mathbf{V}_{ex}$ is the vector sum of all extra components [the only extra component suggested so far is that caused by a hypothesized explosive origin of a void (98, 133)]. The components $\mathbf{V}_{vir}$ and $\mathbf{V}_{in}$ are discussed in detail elsewhere (cf. 54, 69), and $\mathbf{V}_H$, $\mathbf{V}_{out}$, and $\mathbf{V}_{ex}$ are discussed below; a previous review with different perspectives is provided by Ostriker (130).

First consider a locally Newtonian, Euclidean, homogeneous, isotropic universe of mass density $\rho_u \simeq 5 \times 10^{-30}$ g cm^{-3} consisting of non-interacting unit point masses (which are henceforth simply called "particles"). The relative velocity V_H of any two particles separated by a distance $R_{ij} \ll c/H_0$ (where c is the vacuum speed of light and H_0 is the local Hubble constant) obeys the Hubble relation $V_H = H_0 R_{ij}$. Now consider a similar universe—the same model except for the presence of a single ellipsoidal void. For simplicity, the mass density of the void, ρ_v, is assumed constant, so that its density deficiency is $\rho_{uv} = \rho_u - \rho_v$. As pointed out, for example, by Icke (97), according to this model the void can be considered as a region of *negative density* in a uniform background. Therefore, a particle located on the perimeter of a void feels an *outward* force that decreases with increasing distance from the void center (cf. 148c, pp. 161–84); consequently, as time passes, asphericities will tend to disappear. In this way, Icke (97) explained analytically an effect that had been observed by Centrella & Melott (36) from a three-dimensional computer simulation of large-scale structure in the Universe. Icke's result was obtained independently by Fujimoto (79), whose extensive model calculations in the framework of an expanding universe are also applied to estimate time scales for achieving sphericity (which he finds are typically $< H_0^{-1}$) and to demonstrate that the neglect of the effect of outfall velocities leads to an overestimate of the radial length of the Boötes void (by a factor of ~ 1.4 according to the model calculations).

Consider a spherical void of radius $R_v \sim 25$ Mpc with a contiguous shell of particles moving outward at the velocity (relative to the Hubble flow and with virial motions removed) given by $\mathbf{V}_{vs} = \mathbf{V}_{in} + \mathbf{V}_{out} + \mathbf{V}_{ex}$. We adopt $\mathbf{V}_{in} \sim 300$ km s^{-1} and determine $\mathbf{V}_{out}$ and $\mathbf{V}_{ex}$ as follows. The acceleration of a particle on the perimeter of the void equals the unbalanced force, $dV_{out}/dt = GM_{uv}/R_v^2 = 4\pi G \rho_{uv} R_v/3$ directed outward from the void, where G is the Newtonian gravitational constant. A crude integration then gives

$V_{out} \approx (GM_{uv}/R_v^2)\ H_0^{-1}$. If $\rho_{uv} = \rho_u$, then $V_{out} \sim 600$ km s^{-1}. The contiguous shell tends toward a sharp structure because points that lie at distances $r > R_v$ experience a Keplerian falloff in outfall velocity ($V_{out} \sim r^{-1/2}$), so that particles nearer the void tend to overtake more distant particles.

An estimate of V_{ex} similar to that by Ostriker (130) is now made. An explosive origin of a void evacuates the mass M_{uv}. The median distance of this material from the center of the void is $\simeq 0.8R_v$. Hence $V_{ex} \approx 0.2R_vH_0^{-1}$. From this relation, for $R_v \sim 25$ Mpc, we obtain $V_{ex} \sim 250$ km s^{-1}. For $M_{uv} = M_u$, the corresponding kinetic energy of the ejected material, $E_{ex} \sim M_{uv}V_{ex}^2/2$, is $E_{ex} \sim 2 \times 10^{63}$ ergs (the energy equivalent of 10^9 solar masses). The source of this large quantity of energy and other problems noted by Oort (128, p. 425) make difficult the creation of voids with a characteristic length of ~ 50 Mpc by this mechanism. Nevertheless, physical processes within blast waves generated in a cosmic explosion may be significant for the formation of galaxies and smaller voids, and details of models within this framework have been worked out (e.g. 34, 98, 99, 130, 174, 210).

From the above discussion, it should be clear that the observed structure and kinematics of voids are consistent with basic theoretical considerations to within the large uncertainties of both the observational data and the theory. The crude analysis presented above is intended both to illustrate some basic aspects of the dynamical evolution of a void and to underline the theoretical need for forthcoming observational results on detailed structural and kinematic parameters of homogeneous samples of voids and their contiguous shells. More sophisticated analyses of the dynamical evolution of voids are given in (26a, 71, 85, 91, 92, 112, 122, 124–126, 139, 143, 144b).

3.2.2 ORIGIN OF VOIDS An excellent introduction to the origin of large-scale structure is provided by Oort (128, pp. 418–25).

It is assumed that the present large-scale structure evolved from fluctuations that occurred in an early era prior to the recombination of hydrogen [28, 76a, 86, 118, 177, 206, 211f, 215c, 218; also cf. Oort (128)]. The primary aim of these theoretical calculations is to generate predictions consistent with all known cosmologically relevant data [e.g. (*a*) the Hubble relation, $V_H = H_0R_{ij}$; (*b*) the presence of the 2.75-K cosmic blackbody radiation, its 600 km s^{-1} dipole anisotropy, and the nondetection of superimposed irregularities; (*c*) the correlation scale length of the space distribution of galaxies (10 Mpc) and clusters of galaxies (50 Mpc); (*d*) the presence of superclusters and voids each with a characteristic length ~ 50 Mpc; and (*e*) the infall velocity of the Local Group within the Local

Supercluster, and other less clearly determined motions]. According to cosmological evolutionary calculations by, for example, Hoffman et al. (91) [see also (29a, 210a)], the density contrasts at recombination required to form the observed voids correspond to predicted irregularities in the cosmic blackbody radiation of characteristic angular size ~ 10 arcmin, which have *not* been observed (cf. Section 2.2.3). This discrepancy could be understood if the irregularities originated after the recombination era by, for example, the cosmic explosions discussed in Section 3.2.1. Alternatively, the irregularities might have originated in the prerecombination era, but their effective amplitude is smaller than inferred from the distribution of galaxies because of the occurrence of biased galaxy formation. This mechanism was suggested by Kaiser (100) and is being studied extensively (cf. 33a, 118a, 144a, 149; S. D. M. White et al., preprint, 1987; A. L. Melott, preprint, 1987).

The model of biased galaxy formation assumes that at a given epoch, the initial density fluctuations [i.e. the spectrum of $\rho(\mathbf{r}) - \langle \rho \rangle$, where $\rho(\mathbf{r})$ is the density at a given location and $\langle \rho \rangle$ is the global average density], can be represented by the superposition of Gaussian functions with a spectrum of amplitudes (A) and wavelengths (λ). It also assumes that galaxies form whenever a density fluctuation exceeds a threshold value (astrophysically determined, but not necessarily known). Consider, for example, a simple model in which most of the mass of the Universe is contained in a Gaussian wave with $\lambda \sim \infty$ (consistent with the smoothness of the sky distribution of the cosmic blackbody radiation), but a small fraction of the mass is in a Gaussian with $\lambda \sim 50$ Mpc (superclusters, voids) and another small fraction is in a Gaussian with $\lambda \sim 5$ Mpc (galaxy clusters). In this model, the peaks above threshold are more clustered than the mass, so that the cluster-cluster correlation scale length is larger than the galaxy-galaxy correlation scale length (cf. Section 2.2.1). In addition, the voids contain matter, so that the predicted cosmic motions are consistent with observational indications (cf. Sections 2.1.4, 2.2.1) and the cosmic blackbody radiation is effectively smooth (cf. Section 2.2.3).

The successes of the biased galaxy model are to be weighed against the ad hoc "save-the-phenomena" nature of its assumptions (a feature that is shared with many cosmological models). Such assumptions are necessitated by a gap in our understanding of fundamentals, which is manifested very noticeably in mass/time-scale problems (cf. Section 4). Cosmological modeling is founded on the postulate that unexplained gravitational effects are caused mainly by dark matter. Efforts to test this hypothesis have led primarily to enigmatic empirical results and logical puzzles that must be resolved before any of the cosmological models developed to explain the observed large-scale structure can be considered to be substantially more

than physically speculative mathematical constructs. These models, nevertheless, do provide logical predictions that can be compared with empirical data, and in this way they supply diagnostic probes that may provide clues to the resolution of the mass/time-scale problems reviewed in Section 4.

4. MASS/TIME-SCALE PROBLEMS

Previous reviews include Faber & Gallagher (69), Rood (156), Ostriker (132), Bekenstein (26), and Trimble (201).

4.1 *Masses*

Newtonian/general relativistic mechanics, with its simple and beautiful foundations, provides a logically consistent explanation of the observed kinematic properties of the members of the solar system. In extragalactic astronomy, however, perplexing inconsistencies exist between observed kinematic properties and theoretical expectations:

1. The following problem in Galactic astronomy seems to be amplified in the extragalactic domain: The application in 1932 by J. H. Oort and more recently (with updated methodology and data) by J. Bahcall (7, and references therein) of Newtonian dynamics to kinematic properties of stellar tracers within about 200 pc of the Sun predicts a mass (the *dynamical* mass $M_{\rm dyn}$) that is a factor of 2 larger than that calculated from a comprehensive accounting of identified stellar, gaseous, and dust material in the solar neighborhood ($M_{\rm id}$). Included in the inventory of identified matter are objects directly observed by means of their electromagnetic signatures and objects plausibly inferred from reasonable extrapolations of data guided by results from the theory of stellar evolution. If we define a mass anomaly index by $x_{\rm m} = M_{\rm dyn}/M_{\rm id} - 1$, i.e. the fractional excess of the dynamical mass relative to the identified mass, then $x_{\rm m} = 0$ for the solar system but $x_{\rm m} \simeq 1$ for the solar neighborhood.

2. The surface luminosity density of the disk of a spiral galaxy can be approximated by an exponential function of radius with a disk scale length of typically $h_{\rm D} \simeq$ a few kiloparsecs. For radii less than approximately $2.5h_{\rm D}$, the observed rotational curve, i.e. rotational velocity (deprojected radial velocity) vs. radius, appears to be consistent with the model characterized by a constant M/L (ratio of mass to luminosity) and a distribution of mass identical to that of light. However, for radii larger than about $2.5h_{\rm D}$, the rotation curve remains flat (constant rotational velocity) up to a limit of approximately $10h_{\rm D}$ (set by the current sensitivity for detection of the 21-cm spectral line of neutral hydrogen). If, within a radius of $2.5h_{\rm D}$,

the dynamical mass and identified mass are assumed to be identical (a conservative assumption), then as the radius is increased, the dynamical mass exceeds the identified mass by larger and larger factors. The matter within $10h_D$ has a mass anomaly of $x_m \simeq 3$. These properties and other regularities and characteristic numerical values of the rotation curves of spiral galaxies are discussed in depth by Bahcall & Casertano (8), van Albada & Sancisi (207), Kent (101, 102), and Athanassoula et al. (6a).

3. Typically, the identified mass of a group of galaxies is well approximated by the sum of the masses of its four or five most luminous members. Operationally, a group is classified as compact or loose according to whether a typical separation of two neighboring group members is a small number of galaxy diameters or $\sim$20 times larger. Williams & Rood (214) recently found that typically $x_m \simeq 15$ for a loose group chosen from an especially carefully determined sample. Using scaling arguments, they then found that typically $x_m \sim 0$ for a compact group selected from the homogeneous and complete sample obtained by Hickson (89). By applying improved data and more sophisticated analytical procedures, P. Hickson (private communication, 1987) obtains dynamical parameters suggesting that typically $x_m \simeq 4$ for compact groups.

4. The Coma cluster contains hundreds of luminous member galaxies and possesses the symmetry and radial distribution of galaxies expected from a system in Newtonian gravitational equilibrium. Therefore, in 1933 Zwicky (219) was surprised to find that the mass of this cluster derived according to these assumptions from kinematic data applied to the virial theorem is much larger than the mass estimated to be contained within its entire galaxy content. In 1936, results for the Virgo cluster by Smith (185) confirmed this effect. Nevertheless, uncertainties in the data and analyses were sufficiently large to engender skepticism about the physical nature of the effect (152). But by 1972, the homogeneity of the data base had improved considerably, recently discovered optically luminous intergalactic material (59a) was added to the inventory of mass contributors, and the analytical techniques were diversified to include model-fitting as well as virial theorem techniques, which all gave consistent results (161). A general agreement developed that the effect is real. Over the last decade, the optical data base continued to improve (102a), and X-ray-emitting intergalactic ionized gas was discovered, which contributes a mass comparable to that contributed by the galaxies themselves (68, 76, 123). Results of the recent comprehensive dynamical analysis by Kent & Gunn (102a) indicate that the mass anomaly index for the Coma cluster is $x_m \sim 15$, a value that is typical for rich clusters. In accordance with results of the discussion by Blumenthal et al. (28), we note that rich clusters and loose groups have similar mass anomaly indices.

5. The values of typical x_m estimated above appear to be related to the class of extragalactic object under study. But even within a given class, available evidence suggests that there is a physical range of x_m. For example, although typically $x_m \sim 15$ for loose groups, Williams (213) finds from accurate data for the six most luminous galaxies in the IC 698 group that $x_m \simeq 0$. Is x_m correlated with other physical properties of an extragalactic object such as radius, velocity dispersion, number of members, number density, mass, or mass density? We have reason to be optimistic that the suggestive results of early work (100c, 157, 159, 159a, 162) will soon be superseded by definitive results made possible by modern computer technology and the accurate and extensive modern data base.

Recently, several new techniques have been introduced to gain information about the distribution of dynamical mass for galaxies with special structural characteristics: (*a*) Some S0 galaxies contain polar rings (which intersect the galactic rotational axis); measurements are being made of kinematic properties of polar rings to determine the angular dependence of the dynamical mass distribution in these galaxies (207a, 212). (*b*) Mass estimates for elliptical galaxies from the broadening of composite stellar spectral lines are uncertain partly because the effective ellipticities of the stellar orbits are unknown. However, the velocity vectors of the particles constituting a gas in thermal equilibrium are isotropic, and some elliptical galaxies reveal themselves in X-ray emission as an ionized gas with a thermal spectrum. Nevertheless, the mass of a galaxy derivable from properties of this gas is sensitive to its radial temperature gradient, which requires a next-generation X-ray detector for accurate measurement (68, 76, 169). (*c*) Some elliptical galaxies contain many shells of matter in their outer parts; Hernquist & Quinn (88) have developed techniques that apply properties of an array of shells to probe the distribution of dynamical mass in the outer parts of these galaxies. (*d*) Structural parameters of low-surface-brightness dwarf galaxies represent extremes that differ considerably from typical structural parameters of the spiral, S0, and elliptical galaxies ordinarily studied. Aaronson (1) determined definitive dynamical masses of dwarf galaxies from accurately determined kinematic properties of samples of well-chosen member stars. (*e*) The gravitational lensing of quasars offers unique possibilities for probing the mass distribution of galaxies and clusters of galaxies at large redshifts [see (132) for references].

Heisler et al. (87) [see also Bahcall & Tremaine (9a)] have presented three alternatives to the virial theorem for estimating the masses of groups of galaxies. The various uncertainties in real data contribute differently to the overall uncertainty in the dynamical masses provided by each of the four mass estimators. As a valuable consistency check, all four techniques

should generally be applied to determine the dynamical mass of a group of galaxies.

Over the last several decades, a large part of the electromagnetic spectrum has become accessible to telescopic observation. This has led to the discovery of neutral and ionized intergalactic gas clouds in small groups of galaxies (14a, 163, 214) and ionized gas in rich clusters (76, 169) in amounts that are small compared with the amounts needed to resolve mass anomalies. After long-term intensive and diversified observational efforts to increase the inventory of identified masses, the mass anomalies continue to remain perplexing and formidable.

4.2 *Survival Times*

The dynamical mass of a system of galaxies may be written as $M = V^2R/G$, where V is an effective rms velocity of the galaxies about the system's barycenter, R is an effective radius (related to the harmonic radius) of the system, and G is the Newtonian gravitational constant. The equation for dynamical mass can be recast as an equation for dynamical time, i.e. $t_{dyn} = R/V = (R^3/GM)^{1/2} = (G\rho)^{-1/2}$, where ρ is an effective density. The time scale for any specified effect of the gravitational interactions of galaxies in a system is simply t_{dyn} multiplied by a dimensionless parameter. For example, a derivation based on fundamentals of galactic dynamics contained in the recent textbook by Binney & Tremaine (27a) implies, in crude approximation, that the time scale to slow the motion of a galaxy appreciably by dynamical friction is simply $t_{df} \sim Nt_{dyn}$, where N is an effective number of galaxies in the system. It follows from this line of reasoning that if derived dynamical masses lead to anomalous observed effects, so too should derived dynamical friction time scales.

In 1975, Tremaine et al. (199) showed that the dynamical friction time scale for globular clusters passing near the center of M31 is much smaller than the age of M31. Thus many of the globular clusters should have spiraled into the nucleus of M31, and their disruption products should now contribute to the mass of the nucleus. The actual fractional contribution is currently uncertain pending further kinematic observations of the nucleus (198b).

The formula for t_{df} adopted by Tremaine et al. is a logical consequence of Newtonian mechanics and follows from the classical derivation by Chandrasekhar (36a) for a test star that experiences random Newtonian gravitational encounters as it moves in an infinite homogeneous field of stars. This formula is consistent with results of N-body simulations by Barnes (21) and an analytical formalism developed by Tremaine & Weinberg (200) for a test star that rotates or revolves through a spherical system.

The latter study indicates that frictional effects arise entirely from near-resonant stars.

In 1977, Hickson et al. (90) pointed out that $t_{df} \sim 0.01\ H_0^{-1}$ (where $H_0^{-1} \sim 2 \times 10^{10}$ yr is the Hubble time scale) for compact groups of galaxies, which measures the survival time of the group members against coalescence by means of dynamical friction. *N*-body simulations of compact groups by Barnes (21) confirm this time scale and depict the mergers graphically. Let $\eta = N_{product}/N_{source}$, where $N_{product}$ is the number of galaxies that are merger products of compact groups in a volume in space containing N_{source} compact groups. Then we can define a dynamical friction time scale anomaly index by $x_\tau = \eta_{dyn}/\eta_{id} - 1$. The parameter η_{dyn} is the value obtained if $N_{product}$ is inferred from the application of the formula for t_{df}, and η_{id} is the value obtained from the observationally identified merger products. For example, if the merger products of compact groups with properties as defined by Hickson (89) are identified with the galaxies having the same range of luminosity in the general luminosity function (a conservative upper limit), and if the formation of compact groups and their coalescence into galaxies (modeled as *immutable* end products) are steady-state processes over the time $t \sim H_0^{-1}$, then $\eta_{dyn} \sim 100$ and $\eta_{id} \sim 10$, so that $x_\tau \sim 10$. [Here the larger estimate of x_τ presented in (214) has been decreased by a factor of 10 with the inclusion of new data and more refined analysis by P. Hickson (private communication, 1987).]

Some of the uncertainties in an analysis for compact groups are not present in an analysis for another class of extragalactic objects—the Abell clusters of Bautz-Morgan type I, I–II (defined to contain a supergiant, most luminous galaxy) as identified by Leir & van den Bergh (112a). These clusters are easy to recognize because the most luminous member, whether a single or binary supergiant galaxy, is much more luminous than any other cluster member. It follows from the theory of dynamical friction that when a binary supergiant galaxy merges, it becomes a single supergiant galaxy. A major advantage of this type of sample is that nearly all of the selection functions are the same for the sources (binary supergiant galaxies) and the products (single supergiant galaxies). It is observed that 25% of BM I, I–II clusters contain binary supergiant galaxies (160). If each single supergiant galaxy is the merger product of a binary supergiant galaxy (a conservative upper limit), and if the formation of binary supergiant galaxies and their coalescence into single supergiant galaxies (modeled as immutable end products) are steady-state processes over the time $t \sim H_0^{-1}$, then it follows that $\eta_{id} = 3$; and because $t_{df} \sim 0.03 H_0^{-1}$ for the merger of a binary supergiant galaxy (160, 211b,d,g), then $\eta_{dyn} \sim 30$, so that $x_\tau \sim 10$. By reestimating values of parameters, the severity of the anomaly could be reduced (198a), but its total elimination appears to

require that single supergiant galaxies are *mutable*, i.e. they often transform into binary supergiant galaxies through the capture of a luminous cluster member. But visual inspection of BM I, I–II clusters suggests that a single supergiant galaxy is immutable in the sense that its capture of the next most luminous cluster member would result in a system identified as a single supergiant galaxy with a satellite, not a binary supergiant galaxy [i.e. the difference in luminosity between a single supergiant galaxy and the next most luminous cluster member is large compared with the difference in luminosity of the components of a binary supergiant galaxy (160)]. This important observational result should be checked both visually by independent observers and photometrically by accurate modern techniques.

A class of Abell clusters has been discovered that contains numerous binary galaxies (188). Research is needed to determine the detailed dynamical structure of these binary galaxies and to identify the structural characteristics or dynamical processes that permit this class of clusters to exist in the presence of the dynamical friction that tends to transform binary galaxies into single galaxies.

4.3 *Explanatory Hypotheses*

Every hypothesis attempting to explain mass anomalies applies one or the other of the following two assumptions: (*a*) Galaxies and systems of galaxies contain enough dark matter in one or more forms that have so far escaped detection to resolve the mass anomaly (132, 201). (*b*) Newtonian/general relativity theory does not apply in extragalactic astronomy (cf. 72, 96a, 110, 119, 153, 168, 168a, 197). A theory is sought that is conceptually elegant and explains all of the mass anomalies without requiring any dark matter. A discussion by Bekenstein (26) describes major difficulties with both dark matter and new physics hypotheses toward explaining the mass anomalies ($x_m > 0$). It seems that the time-scale anomalies ($x_\tau > 0$), if they survive the detailed observational and theoretical scrutiny that they deserve, would create even more difficulties for both classes of hypotheses.

A plausibility argument in favor of dark-matter hypotheses is that the known physical laws allow many different ways in which matter could escape detection by modern detectors. A plausibility argument in favor of a new physical law is that the forces relevant to a given system tend to correlate with its mass density. For example, atomic nuclei and the solar system have vastly different mass densities. Measured on scales that are physically useful in other applications, the mass densities appropriate to a galaxy and a system of galaxies are much closer to the cosmological density than to the density of the solar system. Another plausibility argument is the following: Qualitative and quantitative descriptions of physical

laws, including Newtonian/general relativistic dynamics, are specified from results of experiments in terrestrial laboratories. Our experience with verifying these laws in and beyond the solar system suggests that they are universal. If, in addition, our inventory of physical laws were complete, then these laws would provide intelligent creatures with the tools they need to understand the physical nature of the cosmos, and their role within it, to the maximum extent that the laws allow. But our ability to *identify* and quantify laws in the laboratory is limited by the range of physical parameters accessible to the laboratory. Therefore, to obtain a complete inventory of physical laws, it may be necessary to examine more fully the experiments performed by nature in the ultimate laboratory, the Universe.

ACKNOWLEDGMENTS

I thank Drs. G. Chincarini, T. L. Page, M. Postman, and M. F. Struble for critically reading an earlier draft of the manuscript and offering valuable suggestions. Significant editorial improvements to the manuscript have been made by Production Editor Keith Dodson and Associate Editor David Layzer. This article was written during a 1986–87 visit at the Institute for Advanced Study; the hospitality of the Faculty in the School of Natural Sciences is gratefully acknowledged. This work is supported in part by the National Science Foundation under grant AST-8513087.

Literature Cited

1. Aaronson, M. 1987. In *Nearly Normal Galaxies*, ed. S. M. Faber, pp. 57–66. New York: Springer-Verlag
1a. Aaronson, M., Bothun, G., Mould, J., Huchra, J., Schommer, R. A., Cornell, M. E. 1986. *Ap. J.* 302: 536
2. Aaronson, M., Huchra, J., Mould, J., Schechter, P. L., Tully, R. B. 1982. *Ap. J.* 258: 64
2a. Aarseth, S. J., Gott, J. R. III, Turner, E. L. 1979. *Ap. J.* 228: 664
3. Aarseth, S. J., Saslaw, W. C. 1982. *Ap. J. Lett.* 258: L7
4. Abell, G. O. 1958. *Ap. J. Suppl.* 3: 211
5. Abell, G. O. 1961. *Astron. J.* 66: 607
6. Andersen, P. H. 1986. *Phys. Today* 11: 17
6a. Athanassoula, E., Bosma, A., Papaioannou, S. 1987. *Astron. Astrophys.* 179: 23
7. Bahcall, J. N. 1986. In *Dark Matter in the Universe, IAU Symp. No. 117*, ed. J. Kormendy, G. R. Knapp, pp. 17–31. Dordrecht: Reidel
8. Bahcall, J. N., Casertano, S. 1985. *Ap. J. Lett.* 293: L7
9. Bahcall, J. N., Joss, P. C. 1976. *Ap. J.* 203: 23
9a. Bahcall, J. N., Tremaine, S. 1981. *Ap. J.* 244: 805
10. Bahcall, N. A. 1977. *Ann. Rev. Astron. Astrophys.* 15: 505
11. Bahcall, N. A. 1985. Paper presented at Tex. Symp. Relativ. Astrophys., 12th, December 1984, Jerusalem
12. Bahcall, N. A. 1986. *Ap. J. Lett.* 302: L41
13. Bahcall, N. A. 1987. *Comments Astrophys.* 11: 283
14. Bahcall, N. A., Burgett, W. S. 1986. *Ap. J. Lett.* 300: L35
14a. Bahcall, N. A., Harris, D. E., Rood, H. J. 1984. *Ap. J. Lett.* 284: L29
15. Bahcall, N. A., Soneira, R. M. 1982. *Ap. J.* 262: 419
16. Bahcall, N. A., Soneira, R. M. 1982. *Ap. J. Lett.* 258: L17
17. Bahcall, N. A., Soneira, R. M. 1983. *Ap. J.* 270: 20
18. Bahcall, N. A., Soneira, R. M. 1984. *Ap. J.* 277: 27
19. Bahcall, N. A., Soneira, R. M., Burgett, W. S. 1986. *Ap. J.* 311: 15

20. Balzano, V. A., Weedman, D. W. 1982. *Ap. J. Lett.* 255: L1
21. Barnes, J. 1985. *MNRAS* 215: 517
22a. Barrow, J. D., Bhavsar, S. P. 1987. *Q. J. R. Astron. Soc.* 28: 109
22b. Barrow, J. D., Bhavsar, S. P., Sonoda, D. H. 1985. *MNRAS* 216: 17
23. Batuski, D. J., Burns, J. O. 1985. *Ap. J.* 299: 5
24. Batuski, D. J., Burns, J. O. 1985. *Astron. J.* 90: 1413
25. Batuski, D. J., Melott, A. L., Burns, J. O. 1987. *Ap. J.* 322: 48
26. Bekenstein, J. D. 1987. *Proc. Can. Conf. Gen. Relativ. Relativ. Astrophys.*, ed. C. Dyer. Singapore: World Scientific. In press
26a. Bertschinger, E. 1985. *Ap. J. Suppl.* 58: 1
27. Bhavsar, S. P., Barrow, J. D. 1983. *MNRAS* 205: 61P
27a. Binney, J., Tremaine, S. 1987. *Galactic Dynamics*, pp. 187–90, 420–27. Princeton, NJ: Princeton Univ. Press
28. Blumenthal, G. R., Faber, S. M., Primack, J. R., Rees, M. J. 1984. *Nature* 311: 517, 313: 72
29. Bok, B. J., Bok, P. F. 1957. *The Milky Way*. Cambridge, Mass: Harvard Univ. Press
29a. Bond, J. R., Efstathiou, G. 1984. *Ap. J. Lett.* 285: L45
30. Bothun, G. D., Beers, T. C., Mould, J. R., Huchra, J. P. 1986. *Ap. J.* 308: 510
31. Bouchet, F. R., Lachiéze-Rey, M. 1986. *Ap. J. Lett.* 302: L37
32. Brosch, N., Gondhalekar, P. M. 1984. *Astron. Astrophys.* 140: L43
33. Brosch, N., Greenberg, J. M. 1983. *Astrophys. Space Sci.* 90: 457
33a. Brown, M. E., Peebles, P. J. E. 1987. *Ap. J.* 317: 588
33b. Burns, J. O., Batuski, J. O. 1987. In *Observational Cosmology, IAU Symp. No. 124*, ed. A. Hewitt, G. Burbidge, L.-Z. Fang, pp. 319–22. Dordrecht: Reidel
34. Carr, B. J., Ikeuchi, S. 1985. *MNRAS* 213: 497
35. Carswell, R. F., Rees, M. J. 1987. *MNRAS* 224: 13P
36. Centrella, J., Melott, A. L. 1983. *Nature* 305: 196
36a. Chandrasekhar, S. 1943. *Ap. J.* 97: 255
37. Chincarini, G. 1978. *Nature* 272: 515
38. Chincarini, G. 1983. In *Early Evolution of the Universe and its Present Structure, IAU Symp. No. 104*, ed. G. O. Abell, G. Chincarini, pp. 159–65. Dordrecht: Reidel
39. Chincarini, G. 1984. In *Astronomy with Schmidt-Type Telescopes, IAU Colloq. No. 78*, ed. M. Capaccioli, pp. 511–26. Dordrecht: Reidel
41. Chincarini, G. L., Giovanelli, R., Haynes, M. P. 1983. *Ap. J.* 269: 13
42. Chincarini, G. L., Giovanelli, R., Haynes, M. P. 1983. *Astron. Astrophys.* 121: 5
43. Chincarini, G., Martins, D. 1975. *Ap. J.* 196: 335
43a. Chincarini, G., Rood, H. J. 1972. *Astron. J.* 77: 4
44. Chincarini, G., Rood, H. J. 1972. *Astron. J.* 77: 448
45. Chincarini, G., Rood, H. J. 1975. *Nature* 257: 294
46. Chincarini, G., Rood, H. J. 1976. *Ap. J.* 206: 30
48. Chincarini, G., Rood, H. J. 1980. *Sky Telesc.* 1980 (May): 364
49. Chincarini, G., Rood, H. J., Thompson, L. A. 1981. *Ap. J. Lett.* 249: L47
50. Coles, P. 1986. *MNRAS* 222: 9P
50a. Collins, C. A., Joseph, R. D., Robertson, N. A. 1986. *Nature* 320: 506
51b. da Costa, L. N., Pellegrini, P. S., Sargent, W. L. W., Tonry, J., Davis, M., et al. 1988. *Ap. J.* In press
53. Davis, M., Geller, M. J., Huchra, J. 1978. *Ap. J.* 221: 1
54. Davis, M., Peebles, P. J. E. 1983. *Ann. Rev. Astron. Astrophys.* 21: 109
55. Dekel, A., West, M. J. 1985. *Ap. J.* 288: 411
56. de Lapparent, V., Geller, M. J., Huchra, J. P. 1986. *Ap. J. Lett.* 302: L1
57. de Lapparent, V., Geller, M. J., Huchra, J. P. 1987. *Proc. Tex. Symp. Relativ. Astrophys., 13th*, ed. M. Ulmer. In press
58. de Vaucouleurs, G. 1953. *Astron. J.* 58: 30
59. de Vaucouleurs, G. 1976. *Ap. J.* 203: 33
59a. de Vaucouleurs, G., de Vaucouleurs, A. 1970. *Astrophys. Lett.* 5: 219
59b. de Vaucouleurs, G., de Vaucouleurs, A., Corwin, H. G. 1976. *Second Reference Catalogue of Bright Galaxies*. Austin: Univ. Tex. Press
59c. Davis, M., Huchra, J., Latham, D. W., Tonry, J. 1982. *Ap. J.* 253: 423
60. Dickel, J. R., Rood, H. J. 1978. *Ap. J.* 223: 391
61. Dickey, J. M., Keller, D. T., Pennington, R., Salpeter, E. E. 1987. *Astron. J.* 93: 788
62. Doroshkevich, A. G., Shandarin, S. F., Zel'dovich, Ya. B. 1982. *Comments Astrophys.* 9: 265
63. Doroshkevich, A. G., Shandarin, S. F., Zel'dovich, Ya. B. 1983. In *Early Evolution of the Universe and its Present Structure, IAU Symp. No. 104*, ed. G.

O. Abell, G. Chincarini, pp. 387–91. Dordrecht: Reidel
63a. Dressler, A. 1984. *Ann. Rev. Astron. Astrophys.* 22: 185
65. Einasto, J., Klypin, A. A., Saar, E. 1986. *MNRAS* 219: 457
67. Ellis, G. F. R., Perry, J. J., Sievers, A. W. 1984. *Astron. J.* 89: 1124
68. Fabbiano, G. 1986. *Publ. Astron. Soc. Pac.* 98: 525
69. Faber, S. M., Gallagher, J. S. 1979. *Ann. Rev. Astron. Astrophys.* 17: 135
69a. Fall, S. M. 1979. *Rev. Mod. Phys.* 51: 21
70. Fall, S. M., Jones, B. J. T. 1976. *Nature* 262: 457
71. Fillmore, J. A., Goldreich, P. 1984. *Ap. J.* 281: 9
72. Finzi, A. 1963. *MNRAS* 127: 21
73. Focardi, P., Marano, B., Vettolani, G. 1983. *Astron. Express* 1(2): 75
76. Forman, W., Jones, C. 1982. *Ann. Rev. Astron. Astrophys.* 20: 547
76a. Frenk, C. S., White, S. D. M., Davis, M. 1983. *Ap. J.* 271: 417
77. Fry, J. N. 1985. *Ap. J.* 289: 10
78. Fry, J. N. 1986. *Ap. J.* 306: 358
78a. Fry, J. N. 1986. *Ap. J.* 306: 366
79. Fujimoto, M. 1983. *Publ. Astron. Soc. Jpn.* 35: 159
79a. Geller, M. J., Huchra, J. P., de Lapparent, V. 1987. In *Observational Cosmology, IAU Symp. No. 124*, ed. A. Hewitt, G. Burbidge, L.-Z. Fang, pp. 301–13. Dordrecht: Reidel
80. Gott, J. R. III, Melott, A. L., Dickinson, M. 1986. *Ap. J.* 306: 341
80a. Gott, J. R. III, Weinberg, D. H., Melott, A. L. 1987. *Ap. J.* 319: 1
81. Gregory, S. A., Thompson, L. A. 1978. *Ap. J.* 222: 784
82. Gregory, S. A., Thompson, L. A. 1982. *Sci. Am.* 246(3): 106
83. Gross, P. G. 1977. *Ap. J.* 215: 417
84. Hamilton, A. J. S. 1985. *Ap. J. Lett.* 292: L35
84a. Hamilton, A. J. S., Gott, J. R. III, Weinberg, D. 1986. *Ap. J.* 309: 1
84b. Haynes, M. P., Giovanelli, R., Chincarini, G. L. 1984. *Ann. Rev. Astron. Astrophys.* 22: 445
85. Hausman, M. A., Olson, D. W., Roth, B. D. 1983. *Ap. J.* 270: 351
86. Heavens, A. 1985. *MNRAS* 213: 143
87. Heisler, J., Tremaine, S., Bahcall, J. N. 1985. *Ap. J.* 298: 8
88. Hernquist, L., Quinn, P. J. 1987. *Ap. J.* 312: 1
89. Hickson, P. 1982. *Ap. J.* 255: 382
90. Hickson, P., Richstone, D. O., Turner, E. L. 1977. *Ap. J.* 213: 323
90a. Hoessel, J. G., Gunn, J. E., Thuan, T. X. 1980. *Ap. J.* 241: 486
91. Hoffman, G. L., Salpeter, E. E., Wasserman, I. 1983. *Ap. J.* 268: 527
92. Hoffman, Y., Shaham, J. 1982. *Ap. J.* 262: L23
92a. Holmberg, E. 1937. *Lund Obs. Ann.* 6: 1
93. Hubble, E. 1936. *The Realm of the Nebulae*. New Haven, Conn: Yale University Press [also 1958. (New York: Dover)]
93a. Huchra, J., Davis, M., Latham, D., Tonry, J. 1983. *Ap. J. Suppl.* 52: 89
94a. Hulsbosch, A. N. M. 1987. *Astron. Astrophys. Suppl.* 69: 439
95. Humphreys, R. M. 1976. *Ap. J.* 206: 114
96. Humphreys, R. M., Pennington, R., Ghigo, F., Dickey, J. 1987. *Visitor Use of the Automated Plate Scanner at the University of Minnesota*. Minneapolis: Dept. Astron., Univ. Minn.
96a. Hut, P. 1981. *Phys. Lett. B* 99: 174
97. Icke, V. 1984. *MNRAS* 206: 1P
98. Ikeuchi, S. 1981. *Publ. Astron. Soc. Jpn.* 33: 211
99. Ikeuchi, S., Tomisaka, K., Ostriker, J. P. 1983. *Ap. J.* 265: 583
99a. Jôeveer, M., Einasto, J. 1978. In *The Large Scale Structure of the Universe, IAU Symp. No. 79*, ed. M. S. Longair, J. Einasto, pp. 241–51
100. Kaiser, N. 1984. *Ap. J. Lett.* 284: L9
100b. Kaiser, N. 1987. *MNRAS* 227: 1
100c. Karachentsev, I. D. 1966. *Astrofizika* 2: 81. Engl. transl., 1967, in *Astrophysics* 2: 39
101. Kent, S. M. 1986. *Astron. J.* 91: 1301
102. Kent, S. M. 1987. *Astron. J.* 93: 816
102a. Kent, S. M., Gunn, J. E. 1982. *Astron. J.* 87: 945
103. Kirshner, R. P., Oemler, A., Schechter, P. L. 1978. *Astron. J.* 83: 1549
104. Kirshner, R. P., Oemler, A., Schechter, P. L. 1979. *Astron. J:* 84: 951
105. Kirshner, R. P., Oemler, A., Schechter, P. L., Shectman, S. A. 1981. *Ap. J. Lett.* 248: L57
106. Kirshner, R. P., Oemler, A., Schechter, P. L., Shectman, S. A. 1987. *Ap. J.* 314: 493
108. Krauss, L. M. 1986. *Sci. Am.* 255(6): 58
109. Krumm, N., Brosch, N. 1984. *Astron. J.* 89: 1461
110. Kuhn, J. R., Kruglyak, L. 1987. *Ap. J.* 313: 1
112. Lake, K., Pim, R. 1985. *Ap. J.* 298: 439
112a. Leir, A. A., van den Bergh, S. 1977. *Ap. J. Suppl.* 34: 381
113a. Lundmark, K. 1927. *Uppsala Medd. No. 30*
113b. Lynden-Bell, D., Faber, S. M.,

Burstein, D., Davies, R. L., Dressler, A., et al. 1988. *Ap. J.* 326: 19
114. MacKay, R. S. 1985. *Proc. Spring Coll. Plasma Phys., Trieste*, ed. W. Grossmann. Singapore: World Scientific. In press
114a. Masson, C. R. 1978. *MNRAS* 185: 9P
115. Materne, J. 1974. *Astron. Astrophys.* 33: 451
116. Mayall, N. U. 1960. *Ann. Astrophys.* 23: 344
117. Melott, A. L. 1980. *Ap. J.* 241: 889
118. Melott, A. L. 1983. *MNRAS* 205: 637
118a. Melott, A. L. 1987. *MNRAS* 228: 1001
119. Milgrom, M. 1983. *Ap. J.* 270: 365
120. Moles, M., del Olmo, A., Perea, J. 1985. *MNRAS* 213: 365
120a. Moody, J. W., Kirshner, R. P., MacAlpine, G. M., Gregory, S. A. 1987. *Ap. J. Lett.* 314: L33
121. Mould, J. 1986. In *Galaxy Distances and Deviations from Universal Expansion*, ed. B. F. Madore, R. B. Tully, pp. 111–16. Boston: Reidel
122. Mücket, J. P. 1985. *Astron. Nachr.* 306: 305
123. Mushotzky, R. F. 1984. *Phys. Scr.* T7: 157
123a. Nilson, P. 1973. *Uppsala General Catalogue of Galaxies. Uppsala Astron. Obs. Ann.*, Vol. 6. Uppsala, Swed: Uppsala Offset Center AB
124. Occhionero, F., Santangelo, P., Vittorio, N. 1983. *Astron. Astrophys.* 117: 365
125. Occhionero, F., Veccia-Scavalli, L., Vittorio, N. 1981. *Astron. Astrophys.* 97: 169
126. Occhionero, F., Veccia-Scavalli, L., Vittorio, N. 1981. *Astron. Astrophys.* 99: L12
126a. Oemler, A. 1974. *Ap. J.* 194: 1
126b. Oemler, A. 1987. In *Nearly Normal Galaxies*, ed. S. M. Faber, pp. 213–19. New York: Springer-Verlag
127. Oort, J. H. 1981. *Astron. Astrophys.* 94: 359
128. Oort, J. H. 1983. *Ann. Rev. Astron. Astrophys.* 21: 373
129. Oort, J. H. 1984. *Astron. Astrophys.* 139: 211
130. Ostriker, J. P. 1986. In *Galaxy Distances and Deviations from the Universal Expansion*, ed. B. F. Madore, R. B. Tully, pp. 273–78. Dordrecht: Reidel
132. Ostriker, J. P. 1987. In *Dark Matter in the Universe, IAU Symp. No. 117*, ed. J. Kormendy, G. R. Knapp, pp. 85–93. Dordrecht: Reidel
133. Ostriker, J. P., Cowie, L. L. 1981. *Ap. J. Lett.* 243: L127
134. Ostriker, J. P., Ikeuchi, S. 1983. *Ap. J. Lett.* 268: L63
135. Otto, S., Politzer, H. D., Preskill, J., Wise, M. B. 1986. *Ap. J.* 304: 62
136. Ozernoj, L. M., Chernomordik, V. V. 1985. *Astron. Tsirk. No. 1407*, p. 1 (In Russian)
137. Ozernoj, L. M., Chernomordik, V. V. 1985. *Astron. Tsirk. No. 1408*, p. 3 (In Russian)
138. Ozernoj, L. M., Chernomordik, V. V. 1986. *Pis'ma Astron. Zh.* 12: 325. Engl. transl. in 1986. *Sov. Astron. Lett.* 12: 135 (From Russian)
139. Palmer, P. L., Voglis, N. 1983. *MNRAS* 205: 543
140. Panek, M. 1985. *MNRAS* 216: 85
141. Pannekoek, A. 1961. *A History of Astronomy*. New York: Interscience
141a. Paturel, G. 1979. *Astron. Astrophys.* 71: 106
142. Peebles, P. J. E. 1974. *Astron. Astrophys.* 32: 197
142a. Peebles, P. J. E. 1980. *The Large-Scale Structure of the Universe*. Princeton, NJ: Princeton Univ. Press
143. Peebles, P. J. E. 1982. *Ap. J.* 257: 438
144. Peebles, P. J. E. 1984. *Science* 224: 1385
144a. Peebles, P. J. E. 1987. *Ap. J.* 317: 576
144b. Peebles, P. J. E. 1987. *Nature* 327: 210
145. Perea, J., Moles, M., del Olmo, A. 1986. *MNRAS* 219: 511
145a. Perea, J., Moles, M., del Olmo, A. 1986. *MNRAS* 222: 49
146. Peterson, B. A. 1970. *Astron. J.* 75: 695
147. Politzer, H. D., Preskill, J. P. 1986. *Phys. Rev. Lett.* 56: 99
148. Postman, M., Geller, M. J., Huchra, J. P. 1986. *Astron. J.* 91: 1267
148a. Postman, M., Huchra, J. P., Geller, M. J. 1986. *Astron. J.* 92: 1238
148c. Ramsey, A. S. 1981. *Newtonian Attraction*. New York: Cambridge Univ. Press
148d. Rees, M. J. 1987. In *Nearly Normal Galaxies*, ed. S. M. Faber, pp. 255–62. New York: Springer-Verlag
149. Rees, M. J. 1985. *MNRAS* 213: 75P
150. Robinson, A. H., Sale, R. D. 1969. *Elements of Cartography*. New York: Wiley
152. Rood, H. J. 1970. *Ap. J.* 162: 333
153. Rood, H. J. 1974. *Ap. J.* 193: 15
153a. Rood, H. J. 1975. *Ap. J.* 201: 551
154. Rood, H. J. 1976. *Ap. J.* 207: 16
155. Rood, H. J. 1979. *Ap. J.* 233: 431
156. Rood, H. J. 1981. *Rep. Prog. Phys.* 44: 1077
157. Rood, H. J. 1982. *Ap. J. Suppl.* 49: 111
158. Rood, H. J. 1983. In *The Nearby Stars and the Stellar Luminosity Function, IAU Colloq. No. 76*, ed. A. G. D. Philip, A. R. Upgren, pp. 411–16. Schenectady, NY: L. Davis Press

158a. Rood, H. J. 1987. *Publ. Astron. Soc. Pac.* 99: 921
159. Rood, H. J., Dickel, J. R. 1978. *Ap. J.* 224: 724
159a. Rood, H. J., Dickel, J. R. 1979. *Ap. J.* 233: 418
160. Rood, H. J., Leir, A. A. 1979. *Ap. J. Lett.* 231: L3
161. Rood, H. J., Page, T. L., Kintner, E. C., King, I. R. 1972. *Ap. J.* 175: 627
162. Rood, H. J., Rothman, V. C. A., Turnrose, B. E. 1970. *Ap. J.* 162: 411
163. Rood, H. J., Williams, B. A. 1985. *Ap. J.* 288: 535
164a. Rubin, V. C. 1977. *Ap. J. Lett.* 211: L1
165. Rubin, V. C., Ford, W. K., Thonnard, N., Roberts, M. S., Graham, J. A. 1976. *Astron. J.* 81: 687
166. Rubin, V. C., Thonnard, N., Ford, W. K., Roberts, M. S. 1976. *Astron. J.* 81: 719
167. Ryden, B. S., Turner, E. L. 1984. *Ap. J. Lett.* 287: L59
167a. Sandage, A., Tammann, G. A. 1981. *A Revised Shapley-Ames Catalog of Bright Galaxies*. Washington, DC: Carnegie Inst. Washington
168. Sanders, R. H. 1984. *Astron. Astrophys.* 136: L21
168a. Sanders, R. H. 1986. *MNRAS* 223: 539
169. Sarazin, C. L. 1986. *Rev. Mod. Phys.* 58: 1
170a. Sargent, W. L. W., Young, P. J., Boksenberg, A., Tytler, D. 1980a. *Ap. J. Suppl.* 42: 41
171. Schaeffer, R. 1985. *Astron. Astrophys.* 144: L1
172. Schechter, P. L. 1980. *Astron. J.* 85: 801
174. Schulman, L. S., Seiden, P. E. 1986. *Ap. J.* 311: 1
175. Schwarzschild, B. 1986. *Phys. Today* 5: 17
176. Shandarin, S. F., Zel'dovich, Ya. B. 1983. *Comments Astrophys.* 10: 33
177. Shapiro, P. R. 1984. In *Clusters and Groups of Galaxies*, ed. F. Mardirossian, G. Giuricin, M. Mezzetti, pp. 447–78. Boston: Reidel
178. Shapley, H. 1957. *The Inner Metagalaxy*. New Haven, Conn: Yale Univ. Press
179. Sharp, N. A. 1981. *MNRAS* 195: 857
180. Shaver, P. A. 1987. *Nature* 326: 773
181. Shectman, S. A., Hiltner, W. A. 1976. *Publ. Astron. Soc. Pac.* 88: 960
182. Silk, J., Szalay, A. S., Zel'dovich, Ya. B. 1983. *Sci. Am.* 249(4): 56
183. Simkin, S. M. 1974. *Astron. Astrophys.* 31: 129
185. Smith, S. 1936. *Ap. J.* 83: 23
186. Soltan, A. 1985. *MNRAS* 216: 537
187. Soneira, R. M., Peebles, P. J. E. 1977. *Ap. J.* 211: 1
187a. Soneira, R. M., Peebles, P. J. E. 1978. *Astron. J.* 83: 845
188. Struble, M. F., Rood, H. J. 1981. *Ap. J.* 251: 471
188b. Struble, M. F., Rood, H. J. 1987. *Ap. J. Suppl.* 63: 555
189. Sunyaev, R. A., Zel'dovich, Ya. B. 1980. *Ann. Rev. Astron. Astrophys.* 18: 537
190. Tanaka, Y. D., Ikeuchi, S. 1983. *Prog. Theor. Phys.* 69: 801
191. Tarenghi, M., Chincarini, G., Rood, H. J., Thompson, L. A. 1980. *Ap. J.* 235: 724
191a. Tarenghi, M., Tifft, W. G., Chincarini, G., Rood, H. J., Thompson, L. A. 1978. In *The Large Scale Structure of the Universe, IAU Symp. No. 79*, ed. M. S. Longair, J. Einasto, pp. 263–66. Dordrecht: Reidel
192. Tarenghi, M., Tifft, W. G., Chincarini, G., Rood, H. J., Thompson, L. A. 1979. *Ap. J.* 234: 793
193. Thuan, T. X., Gott, J. R. III, Schneider, S. E. 1987. *Ap. J. Lett.* 315: L93
196. Tifft, W. G., Gregory, S. A. 1976. *Ap. J.* 205: 696
196a. Tifft, W. G., Gregory, S. A. 1978. In *The Large Scale Structure of the Universe, IAU Symp. No. 79*, ed. M. S. Longair, J. Einasto, pp. 267–70
197. Tohline, J. E. 1983. In *Internal Kinematics and Dynamics of Galaxies, IAU Symp. No. 100*, ed. E. Athanassoula, pp. 205–6. Dordrecht: Reidel
197a. Tonry, J., Davis, M. 1979. *Astron. J.* 84: 1511
198. Totsuji, H., Kihara, T. 1969. *Publ. Astron. Soc. Jpn.* 21: 221
198a. Tremaine, S. 1981. In *The Structure and Evolution of Normal Galaxies*, ed. S. M. Fall, D. Lynden-Bell, pp. 67–84. Cambridge: Cambridge Univ. Press
198b. Tremaine, S., Ostriker, J. P. 1982. *Ap. J.* 256: 435
199. Tremaine, S., Ostriker, J. P., Spitzer, L. 1975. *Ap. J.* 196: 407
200. Tremaine, S. D., Weinberg, M. D. 1984. *MNRAS* 209: 729
201. Trimble, V. 1987. *Ann. Rev. Astron. Astrophys.* 25: 425
201a. Tully, R. B. 1980. *Ap. J.* 237: 390
202. Tully, R. B. 1982. *Ap. J.* 257: 389
203. Tully, R. B. 1982. *Sky Telesc.* 63(June): 550
204. Tully, R. B. 1986. *Ap. J.* 303: 25
204a. Tully, R. B. 1987. *Ap. J.* 323: 1
205. Turner, E. L., Gott, J. R. III. 1975. *Ap. J. Lett.* 197: L89

205a. Turner, E. L., Gott, J. R. III. 1976. *Ap. J. Suppl.* 32: 409
205b. Turner, E. L., Aarseth, S. J., Gott, J. R. III, Blanchard, N. T., Mathieu, R. D. 1979. *Ap. J.* 228: 684
206. Umemura, M., Ikeuchi, S. 1986. *Astrophys. Space Sci.* 119: 243
206a. Vader, J. P., Simon, M. 1987. *Astron. J.* 94: 636
207. van Albada, T. S., Sancisi, R. 1986. *Philos. Trans. R. Soc. London A* 320: 447
207a. van Gorkom, J. H., Schechter, P. L., Kristian, J. 1987. *Ap. J.* 314: 457
207b. Vettolani, G., de Souza, R., Chincarini, G. 1986. *Astron. Astrophys.* 154: 343
208. Vettolani, G., de Souza, R., Marano, B., Chincarini, G. 1985. *Astron. Astrophys.* 144: 506
209. Vettolani, G., de Souza, R. E., Marano, B., Chincarini, G. 1985. *Mem. Soc. Astron. Ital.* 56: 717
210. Vishniac, E. T., Ostriker, J. P., Bertschinger, E. 1985. *Ap. J.* 291: 399
210a. Vittorio, N., Silk, J. 1984. *Ap. J. Lett.* 285: L39
210b. Waldrop, M. M. 1986. *Science* 233: 1386
210c. Weedman, D. W. 1976. *Ap. J.* 203: 6
211. Weinberg, D. H., Gott, J. R. III, Melott, A. L. 1987. *Ap. J.* 321: 2
211b. White, S. D. M. 1978. *MNRAS* 184: 185
211c. White, S. D. M. 1979. *MNRAS* 186: 145
211d. White, S. D. M. 1979. *MNRAS* 189: 831
211e. White, S. D. M. 1984. Talk presented at Inner Space/Outer Space Meet., Fermilab, Ill.
211f. White, S. D. M., Frenk, C. S., Davis, M., Efstathiou, G. 1987. *Ap. J.* 313: 505
211g. White, S. D. M., Sharp, N. A. 1977. *Nature* 269: 395
212. Whitmore, B. C., McElroy, D. B., Schweizer, F. 1987. *Ap. J.* 314: 439
212a. Wilkinson, D. T. 1986. *Science* 232: 1517
213. Williams, B. A. 1983. *Ap. J.* 271: 461
214. Williams, B. A., Rood, H. J. 1987. *Ap. J. Suppl.* 63: 265
215. Zel'dovich, Ya. B. 1970. *Astron. Astrophys.* 5: 84
215a. Zel'dovich, Ya. B. 1973. *Astrofizika* 6: 164
215b. Zel'dovich, Ya. B. 1978. In *The Large Scale Structure of the Universe, IAU Symp. No. 79*, ed. M. S. Longair, J. Einasto, pp. 409–22. Dordrecht: Reidel
215c. Zel'dovich, Ya. B. 1982. *Sov. Astron. Lett.* 8(2): 102
216. Zel'dovich, Ya. B., Einasto, J., Shandarin, S. F. 1982. *Nature* 300: 407
217. Zel'dovich, Ya. B., Novikov, I. D. 1975. *The Structure and Evolution of the Universe.* Moscow: Nauka. Engl. transl. in *Relativistic Astrophysics*, Vol. 2. Chicago: Univ. Chicago Press (From Russian)
218. Zel'dovich, Ya. B., Shandarin, S. F. 1982. *Sov. Astron. Lett.* 8(2): 67
219. Zwicky, F. 1933. *Helv. Phys. Acta* 6: 110
219a. Zwicky, F. 1957. *Morphological Astronomy.* Berlin: Springer-Verlag
220. Zwicky, F., Herzog, E., Karpowicz, M., Kowal, C. T., Wild, P. 1960–1968. *Catalogue of Galaxies and of Clusters of Galaxies*, Vols. 1–6. Pasadena: Calif. Inst. Technol.